Detection of Nonlinear Picosecond Acoustic Pulses by Time-Resolved Brillouin Scattering

Vitalyi E. Gusev

LAUM, UMR-CNRS 6613, Université du Maine, Avenue O. Messiaen,

72085 Le Mans, France

vitali.goussev@univ-lemans.fr

Abstract

In time-resolved Brillouin scattering (also called picosecond ultrasonic interferometry), the time evolution of the spatial Fourier component of an optically excited acoustic strain distribution is monitored. The wave number is determined by the momentum conservation in photon-phonon interaction. For linear acoustic waves propagating in an homogeneous medium, the detected time-domain signal of the optical probe transient reflectivity shows a sinusoidal oscillation at a constant frequency known as the Brillouin frequency. This oscillation is a result of heterodyning the constant reflection from the sample surface with the Brillouin-scattered field. Here, we present an analytical theory for the nonlinear reshaping of a propagating, finite amplitude picosecond acoustic pulse which results in a time-dependence of the observed frequency. In particular, we examine the conditions under which this information can be used to study the time-evolution of the weak-shock front speed. Depending on the initial strain pulse parameters and the time interval of its nonlinear transformation, our theory predicts the detected frequency to either be monotonically decreasing or oscillating in time. We support these theoretical predictions by comparison with available experimental data. In general we find that picosecond ultrasonic interferometry of nonlinear acoustic pulses provides access to the nonlinear acoustic properties of a medium spanning most of the GHz frequency range.

1. Introduction

In picosecond laser ultrasonics ultrashort optical pulses (typically of hundreds of femtoseconds duration) are used both to generate and to detect coherent acoustic pulses.[1,2] In particular, the so-called, picosecond acoustic interferometry[1,3,4] is a powerful opto-acousto-optical method of nondestructive testing and evaluation of optically transparent materials in the GHz-range of acoustic frequencies. It consists in the generation of a picosecond acoustic pulse by a femtosecond laser pulse through laser action on light absorbing optoacoustic transducer and subsequent monitoring of the propagation of this acoustic pulse in the bulk of the transparent material by time-resolved reflectivity measurements. This is possible because of the interaction between the probe femtosecond laser pulse with picosecond acoustic pulses due to the acousto-optic effect. Governed dominantly by the law of the momentum conservation in the photons interaction with acoustic phonon, *i.e.*, in the Brillouin scattering, picosecond ultrasonic interferometry also called time-resolved Brillouin scattering[7], monitors the time evolution of the spatial Fourier component of an optically excited acoustic strain distribution with wave number $\vec{q} = \Delta\vec{k}$. Here, $\Delta\vec{k}$ is the modification of the optical light wavevector in the probed medium. In the small-amplitude limit, a picosecond acoustic pulse propagates at a constant velocity, c_0, without nonlinear changes to its shape. The detected time-domain signal of the optical probe transient reflectivity $dR(t)/R$, which includes a constant reflection from a sample surfaces/interfaces against which the Brillouin-scattered field is heterodyned (Fig. 1), shows a sinusoidal oscillation at a constant cyclic frequency $\omega_{dR/R}$ equal to the Brillouin cyclic frequency $\omega_B = qc_0$. With $\Delta\vec{k}$ known, the measurement allows determination of the velocity $c_0(\omega_B)$ of acoustic phonons at frequency ω_B.

Measuring sound velocity through the Brillouin frequency detection provides additional information necessary for the determination of the thickness of thin transparent layers in picosecond ultrasonics[8,9], where the detection either of the arrival times of the subsequent acoustic echoes[1,3] or the subsequent times of the abrupt amplitude and/or phase variation of the Brillouin signal[7,10,11] provides opportunity to determine the ratio of the film thickness to the sound velocity, but not separately the film thickness and the sound velocity. Time-resolved Brillouin scattering experiments have been extended for the measurements of the velocity of shear hypersound[12]. Performing picosecond ultrasonic interferometry at two different angles of probe incidence it is possible to determine simultaneously the sound velocity and the optical refractive index of the transparent material[13,14]. Recently time-resolved Brillouin scattering experiments has been conducted in spatially inhomogeneous media[7,15]. By measuring how the Brillouin frequency varies with the time delay of the probe laser pulse, i.e., with the propagation time of the acoustic pulse, it is possible to determine with nanometers scale spatial resolution the in-depth variation of sound velocity in the material[7,15]. By performing measurements at few angles of probe incidence, it is possible to determine simultaneously the in-depth profiles of both sound velocity and of the optical refractive index[15]. Moreover from the measurements of the variations in time of the Brillouin signal amplitude it has been possible to determine the spatial profile of the distribution of the photoelastic modulus.[15] Recently developed theory[16] has predicted important advantages that would be achieved with this new technique of the nanoscale in-depth imaging if the amplitude and the phase of the transient optical reflectivity are monitored simultaneously using ultrafast time-resolved optical interferometry[17,18], which provides opportunity to separate precisely through measurements, and not by numerical signal processing, the time-varying amplitude and the time-varying frequency of the Brillouin signal. The perspectives of combining measurements with s-polarized and p-polarized laser probes has been also discussed.[16] Under the particular circumstances, for example for the depth-profiling of the shear rigidity of nanomaterials, it would be advantageous to monitor the Brillouin scattering from the propagating nanoacoustic pulses by time-resolved ultrafast optical polarimetry.[19-22]

Here we develop the theory of the time-resolved Brillouin scattering from the nonlinear coherent picosecond acoustic pulses, i.e., from the acoustic pulses of the finite and not of the infinitely small amplitude.[23] In such pulses nonlinear elastic interactions between different components of the wide-frequency-band spectrum are important at the temporal/spatial scales of the experimental observation. These synchronous acoustic interactions lead to the nonlinear transformation of the picosecond acoustic pulse profile and the formation of the so-called weak shock front or several weak shock fronts, depending on the initial profile of the laser-generated picosecond acoustic pulse. We present an analytical theory describing how nonlinear reshaping of a propagating, finite amplitude picosecond acoustic pulse results in a time-dependence of the observed frequency $\omega_{dR/R}(t) \equiv \omega_B(t)$. In particular, we establish the conditions under which $\omega_{dR/R}(t) = q\upsilon_{sh}(t)$ where $\upsilon_{sh}(t)$ is time-evolving speed of the weak-shock front that can be formed through the nonlinear acoustic transformation of the picosecond strain pulse. Depending on the parameters of the initial picosecond strain pulse and the monitored time interval of its nonlinear transformation, our theory predicts the frequency $\omega_{dR/R}(t) \equiv \omega_B(t)$ to either be monotonically decreasing or oscillating in time. As the weak shock velocity depends on the nonlinear acoustic parameter of the material then the time-resolved Brillouin scattering provides access to the measurements of the acoustic nonlinearity in the GHz frequency range. The possible influence of the linear absorption of acoustic waves on the nonlinear Brillouin frequency is also analyzed. The theoretical predictions are compared with the available experimental results for the bipolar[24] and uni-polar[25] nonlinear acoustic pulses.

It is worth underlining, starting from here in the Introduction, that in general the technique of time-resolved Brillouin scattering monitors the dynamics of a particular spatial Fourier component of the acoustic field and not of a particular frequency of the acoustic field. Only in the case of the linear acoustic field the measurements provide information on the velocity of the acoustic phonon with the wave-number equal to this particular spatial Fourier component (and with the frequency equal to this particular Brillouin frequency). In the case of the nonlinear acoustic fields it is not the case. The theory predicts that the detected frequency in the case of light scattering by nonlinear picosecond acoustic pulses is time-dependent and the experiments are providing information rather on the nonlinear phenomena in the complete frequency spectrum of the acoustic pulse than on the material elastic nonlinearity at a single time-dependent measured frequency. This is because the nonlinear variations in the pulse profile and, consequently, in its spatial Fourier spectrum are due to the interaction between all the spectral components of the acoustic pulse. The frequency of the detected oscillating component in transient reflectivity depends not only on the amplitude of this spectral component but also on the amplitudes and relative phases of the other components of the spectrum. The most obvious illustration of this statement is the case where the detected oscillation frequency is proportional to the velocity of the shock front, which is controlled by the amplitude of the acoustic pulse and not by the amplitude of a particular frequency component. In general, if the initial amplitude of the Brillouin frequency component is the same in two nonlinear acoustic pulses of the different profiles (of the different spectra) the variation in time of the measured frequency will be different. In other words, picosecond ultrasonic interferometry does not monitor the nonlinear self-action of a particular time-dependent frequency component, but nonlinear multi-frequency, multi-scattering acoustic processes in picosecond elastic pulses. Thus, picosecond ultrasonic interferometry of nonlinear acoustic pulses provides access to the nonlinear acoustic properties of a medium covering most of the GHz frequency range.

The article is structured as follows. In Section 2 we remind the backgrounds of signal formation and description in picosecond ultrasonic interferometry (time-resolved Brillouin scattering). Section 3 is devoted to presentation of theory developed for the case when the acoustic signals, probed by picosecond ultrasonic interferometry, are nonlinear. In particular, in Section 3.1 the transient optical reflectivity signals are predicted at the times scales preceding the formation of weak shock front in a uni-polar nonlinear acoustic pulse. In Section 3.2 the manifestations in the transient reflectivity signals of the formation and propagation of infinitely thin shock fronts are described (regime of high acoustic Reynolds numbers). The theory presented in Section 3.3 accounts for the finite duration of the weak shock fronts caused by the frequency-dependent absorption of the hypersound. In Section 3.4 a particular case of transient broadening of weak shock fronts, initially generated by ultrafast laser action, is analyzed. Section 3.5 is devoted to the analytical description of the Brillouin signals in a most general case of multi-polar acoustic pulses and arbitrary acoustic Reynolds numbers. Finally in Section 3.6 an important particular case of symmetric bipolar acoustic pulses is studied in more details. Section 4 presents two applications of the developed theory to the analysis of the available experimental results. In Section 4.1 we interpret earlier reported experimental results obtained by spatially resolved Brillouin scattering technique. In Section 4.2 we use the derived theoretical formulas for the analysis of the available experimental results obtained by time-resolved Brillouin scattering technique. The conclusions are summarized in Section 5.

2. Picosecond ultrasonic interferometry of coherent acoustic pulses

In picosecond laser ultrasonics ultrashort probe laser pulses are scattered by laser- generated picosecond acoustic pulses due to the acousto-optic effect.[6,26,27] Thus, by monitoring the reflected light, the information on the picosecond acoustic pulses can be obtained.[1] In the most of the experiments the transient relative changes $dR(t)/R$ in the intensity of the reflected probe light are detected, where R is the sample reflectivity in the absence of pump laser action. The optical intensity reflectivity R and electromagnetic field reflectivity r are related by

$$dR(t)/R = 2\,\mathrm{Re}[dr(t)/r]\,. \qquad (1)$$

The contribution to this signal, which is caused by acousto-optic interaction of plane collinearly propagating acoustic and light waves in isotropic medium, is proportional to the photo-elastic (acousto-optic) coefficient and the overlap integral of the acoustic strain field with the optical field sensitivity function.[1] The integral is over complete volume probed by the light and the sensitivity function depends on the specific geometry of light scattering in the sample in the absence of the laser-generated coherent acoustic waves.[1,5,10] In particular, when the light normally incident on the sample probes the propagation of the acoustic pulse in optically homogeneous half space (Fig. 1) the photo-elastic contribution to Eq. (1) is given by

$$\frac{dr}{r} = -iC\int_0^{\infty} \eta_{zz}(t,z)e^{i2kz}dz\,, \tag{2}$$

where C is the known complex constant[1,5,10], $\eta_{zz}(t,z)$ is the strain field in the longitudinal acoustic wave propagating along the z axis and k is the complex wave number of the probe light in the medium. In accordance with Eq. (2) the time-resolved measurement of the reflectivity provides information on the evolution in time of the Laplace component of the acoustic field with the complex-valued Laplace parameter $p = -i2k$.[5] The solution in Eq. (2) is particularly simple, when the strain field is composed of the coherent waves propagating in one direction. For example, the strain pulse propagating in the positive direction of z axis can be presented in the form

$$\eta_{zz}(t,z) \equiv \eta_{zz}(t,\xi = z - c_0 t) = \frac{1}{2\pi}\int_{-\infty}^{+\infty}\tilde{\eta}_{zz}(t,q)e^{-iq\xi}dq\,. \tag{3}$$

Here c_0 is the velocity of the linear acoustic waves, i.e., the velocity of the acoustic waves of the infinitely small amplitude, and $\tilde{\eta}_{zz}(t,q)$ describes slow evolution with time of the spatial Fourier spectrum of the coherent acoustic pulse. Note that $\xi = z - c_0 t$ is the moving spatial co-ordinate, and, so, the slow time t in $\eta_{zz}(t,\xi)$ and in $\tilde{\eta}_{zz}(t,q)$ describes the evolution of the strain field in the co-ordinate frame moving with linear sound velocity. When the strain pulse (3) is completely inside the probe half-space $z \ge 0$, i.e., when the value $\eta_{zz}(t, z = 0)$ predicted by Eq. (3) is negligible, the integration in Eq. (2) can be extended to complete space

$$\frac{dr}{r} = -iC\int_{-\infty}^{+\infty}\eta_{zz}(t,z)e^{i2kz}dz\,. \tag{4}$$

In the optically transparent medium the value of k is real, and, thus, Eq. (4) predicts that the time-resolved measurements of the reflectivity monitor the evolution in time of the component of spatial Fourier spectrum of the acoustic wave with the wave number q equal twice the optical wave number. The substitution of Eq. (3) into Eq. (4) results in

$$\frac{dr}{r} = -iC\tilde{\eta}_{zz}(t, q = 2k)e^{i2kc_0t} . \tag{5}$$

The relation $q = 2k$ is a well-known result of the momentum conservation in back-scattering of photon by phonon[6,27]. Thus, mathematically, it is the spatial Fourier transform that ensures the momentum conservation in the photons-phonon interaction. Because of the relation $q \equiv \omega / c_0$, where ω is the cyclic frequency, it is common to say that time resolved reflectivity measurements monitor the time dynamics of the spectral Fourier component of the coherent acoustic field at frequency $\omega = 2kc_0 \equiv \omega_B$, which is known as the Brillouin frequency or the Brillouin frequency shift of the light scattered by acoustic phonon. The measurement of the Brillouin frequency provides opportunity to find the acoustic velocity in the material through the relation $c_0 = \omega_B /(2k)$. These statements can be straightforward verified by presenting the strain pulse in the form

$$\eta_{zz}(t, z) \equiv \eta_{zz}(t, \tau = t - z / c_0) = \frac{1}{2\pi}\int_{-\infty}^{+\infty}\tilde{\eta}_{zz}(t, \omega)e^{i\omega\tau}d\omega , \tag{6}$$

where $\tau = t - z / c_0$ is the so-called retarded time[5] and $\tilde{\eta}_{zz}(t, \omega)$ is the slowly varying in time Fourier frequency spectrum of the acoustic pulse. Substitution of Eq. (6) into Eq. (4) results in

$$\frac{dr}{r} = -iC\tilde{\eta}_{zz}(t, \omega = \omega_B)e^{i\omega_B t} . \tag{7}$$

The solution in Eq. (7), which is equivalent to one in Eq. (5), confirms that time-resolved measurements of the probe light intensity reflectivity (see Eq. (1)) provide access to the detection of coherent acoustic waves at the Brillouin frequency. This is the reason to call this domain of picosecond laser ultrasonics not only “picosecond ultrasonic interferometry”[1] but also sometimes to call it “time-resolved Brillouin scattering”[7]. However the fact, that the Brillouin frequency can be measured using time-resolved variations of the optical reflectivity caused by laser-generated coherent acoustic fields, does not mean that, by measuring the frequency of the oscillations in the $dR(t)/R$ signal, we get exactly the Brillouin frequency $\omega_B \equiv 2kc_0$. By separating the amplitude and the phase in the complex C and $\tilde{\eta}_{zz}(t,\omega)$, i.e., $C = A_C \exp(i\varphi_C)$, $\tilde{\eta}_{zz}(t,\omega_B) = A_\eta(t)\exp\lfloor i\varphi_\eta(t)\rfloor$, and substituting Eq. (7) into Eq. (1), we derive

$$dR(t)/R = 2A_C A_\eta \sin(\omega_B t + \varphi_\eta + \varphi_C)\,. \qquad (8)$$

From Eq. (8) it follows that the transient reflectivity signal induced by photoelasticity oscillates at frequency

$$\omega_{dR/R} = \partial(\omega_B t + \varphi_\eta + \varphi_C)/\partial t = \omega_B + \partial\varphi_\eta/\partial t\,, \qquad (9)$$

which is, in the general case, different from the Brillouin frequency defined above, i.e., $\omega_{dR/R} \neq \omega_B$.

Below we will evaluate $\omega_{dR/R}$ in the particular case where the time-resolved Brillouin scattering is applied for the monitoring the propagation of the nonlinear acoustic pulses. We will describe what information can be extracted from the measurements of $\omega_{dR/R}$. In particular, it will be demonstrated that under some conditions $\omega_{dR/R}/(2k) = (\omega_B + \partial\varphi_\eta/\partial t)/(2k) = c_0 + (1/(2k))\partial\varphi_\eta/\partial t$ provides the information on the velocity of the weak shock front in the profile of the coherent acoustic pulse. It will be also discussed how the parameter of the acoustic nonlinearity of the medium could be accessed through time-resolved Brillouin experiments.

Below we will show that $\partial\varphi_\eta/\partial t$ could be non-zero and could provide non-zero contribution to the experimentally measured $\omega_{dR/R}$ because of the elastic nonlinearity of the tested medium. So it is tentative to call $\omega_{dR/R} = \omega_B + \partial\varphi_\eta/\partial t$ just the time-dependent nonlinear Brillouin frequency $\omega_{dR/R} = \omega_B + \partial\varphi_\eta/\partial t \equiv \omega_B(t)$ (or nonlinear frequency shift). In principle this terminology is acceptable. However, when using this terminology it should not be forgotten that linear Brillouin frequency ω_B is the characteristic of the tested material, which does not depend on the parameters of the monitored picosecond acoustic pulse, while, as it will be demonstrated below, $\partial\varphi_\eta / \partial t$ and consequently also $\omega_{dR/R}$ depend additionally on the temporal profile, i.e. on the complete frequency spectrum, of the monitored picosecond strain pulse.

3. Picosecond ultrasonic interferometry of nonlinear acoustic pulses

Propagation of plane longitudinal acoustic pulses of finite amplitude is controlled in the frame of quadratic approximation of the nonlinear acoustics[23] by the Burgers equation

$$\frac{\partial \upsilon}{\partial t} + \varepsilon\upsilon \frac{\partial \upsilon}{\partial \xi} - \frac{b}{2\rho_0}\frac{\partial^2 \upsilon}{\partial \zeta^2} = 0\,. \tag{10}$$

Here $\upsilon(t, \xi = z - c_0 t)$ describes slow evolution in time of the profile of the particle velocity, which is evaluated in the sonic coordinate frame. This evolution takes place due to the effects of quadratic nonlinearity, which are accounted by the second term in Eq. (10), where ε is the nonlinear acoustic parameter[23], and due to sound absorption proportional to square of frequency, which is accounted by the third term in Eq. (10), where b is the effective viscosity[5] and ρ_0 is the equilibrium density. The dispersion of the acoustic velocity is neglected in Eq. (10).

Let us first present a simple particular example demonstrating the inequality $\omega_{dR/R} \neq \omega_B$ for the nonlinear acoustic pulses described by Eq. (10). We note preliminary that, because particle velocity and the longitudinal strain are related to particle displacement u in the acoustic wave by $\upsilon = \partial u / \partial t$ and $\eta_{zz} = \partial u / \partial z$, respectively, their relation in the moving coordinate frame is $\upsilon \cong -c_0\eta_{zz}$. So

$$\tilde{\eta}_{zz}(t, q = 2k) = -\frac{1}{c_0}\int_{-\infty}^{\infty} \upsilon(t,\xi) e^{i2k\xi} d\xi\,. \tag{11}$$

This relation will be used in the following for the evaluation of the amplitude and the phase of the complex strain spectrum $\tilde{\eta}_{zz}(t, q = 2k)$ entering the solution for transient reflectivity in Eq. (8) and Eq. (9). Without loss of generality it can be considered that the acoustic pulse is located around $\xi = 0$, i.e., around $z = c_0 t$. Then for the short acoustic pulses with the spatial length $l_a(t)$, satisfying the inequality $2kl_a(t) << 1$, i.e., $l_a(t) << \lambda/(4\pi)$, where λ is the optical wavelength in the medium, Eq. (11) can be approximated by

$$\tilde{\eta}_{zz}(t, q = 2k) \approx -\frac{1}{c_0}\int_{-\infty}^{\infty} \upsilon(t,\xi)(1 + 2ik\xi)d\xi \approx -\frac{S}{c_0}\exp\left[i\frac{2k}{S}\int_{-\infty}^{\infty} \upsilon(t,\xi)\xi d\xi\right], \tag{12}$$

where $S \equiv \int_{-\infty}^{\infty} \upsilon(t,\xi)d\xi$ denotes the "surface area" of the acoustic pulse velocity profile, which is known to be constant in nonlinear acoustics due to acoustic momentum conservation.[23] The obtained relation (12) demonstrates that, as far as the profile of the acoustic pulse changes in time, i.e., $\partial\upsilon/\partial t \neq 0$, the phase of the complex strain could contain a time-dependent part $\frac{2k}{S}\int_{-\infty}^{\infty} \upsilon(t,\xi)\xi d\xi$ and $\omega_{dR/R} \neq \omega_B$ could hold. Moreover, using the Burgers equation (10) and applying the integration by parts, the deviation of $\omega_{dR/R}$ from ω_B can be reduced to the form

$$\omega_{dR/R} - \omega_B \approx \frac{2k}{S}\int_{-\infty}^{\infty} \frac{\partial\upsilon(t,\xi)}{\partial t}\xi d\xi = \frac{2k}{S}\int_{-\infty}^{\infty}\left[-\varepsilon\upsilon\frac{\partial\upsilon}{\partial\xi} + \frac{b}{2\rho_0}\frac{\partial^2\upsilon}{\partial\zeta^2}\right]\xi d\xi = \frac{\varepsilon k}{S}\int_{-\infty}^{\infty}\upsilon^2 d\xi\,. \tag{13}$$

In the derivation of the final result in Eq. (13) we have used the condition of the absence of the acoustic field at $\xi = \pm\infty$. The solution in Eq. (13) demonstrates that the deviation of the measured frequency $\omega_{dR/R}$ from the Brillouin frequency ω_B is caused only by the acoustic nonlinearity, i.e., is absent in the absence of nonlinear processes (in case $\varepsilon = 0$). In the absence of nonlinearity linear absorption does not induce the difference between $\omega_{dR/R}$ and ω_B . In the particular case of short acoustic pulses $\omega_{dR/R} - \omega_B$ is proportional to the ratio acoustic pulse energy and the acoustic pulse momentum $\omega_{dR/R} - \omega_B \approx \varepsilon k\int_{-\infty}^{\infty}\upsilon^2 d\xi / \int_{-\infty}^{\infty}\upsilon d\xi$. This relation indicates that $\omega_{dR/R} - \omega_B$ could contain information on the product $\varepsilon\upsilon_a$ of the parameter ε of the acoustic nonlinearity and the characteristic amplitude υ_a of the particle velocity in the strain pulse.

In the general case of the acoustic pulse characterized by the spatial length l_a, i.e., the duration $\tau_a = l_a / c_0$, and the amplitude υ_a, the evolution of the pulse profile predicted by Eq. (19) is known to be controlled by the parameter $\varepsilon\,\mathrm{Re}$, where the notation Re is introduced for the so-called acoustic Reynolds number[23] $\mathrm{Re} \equiv 2\rho_0 c_0 \upsilon_a \tau_a / b$. If the introduced parameter is small, $\varepsilon \mathrm{Re} << 1$, then the dissipation dominates over the nonlinearity, and the nonlinear corrections to the acoustic pulse profile are small and can be taken into account by the method of the successive approximations starting from the solution of the linearized Eq. (10). Moreover if the parameter $\varepsilon \mathrm{Re}$ is small in the initial instance of time $t = 0$, then it will be small later, and the nonlinear effects will be small over complete observation time[23]. This simple regime of acoustic pulse propagation is not of prime interest of our investigation and is not discussed below in details. We are interested here in the analysis of the situation, when initially the nonlinear effects dominate, i.e., $\varepsilon \mathrm{Re}(t = 0) >> 1$, and in the first approximation the evolution of the pulse profile can be described neglecting in Eq. (10) the absorption, i.e. by the so-called simple-wave equation[23]

$$\frac{\partial \upsilon}{\partial t} + \varepsilon \upsilon \frac{\partial \upsilon}{\partial \xi} = 0 . \qquad (14)$$

It is known, however, that in this case the nonlinearity leads to the formation of the so-called weak shock fronts in the profile of the acoustic pulse[23]. The duration of the shock front $\tau_{sh}(t)$ can be much shorter than the initial duration of the acoustic pulse. It means that the profile of the acoustic pulse can not be characterized by a single characteristic time. In the process of the shock steepening the local acoustic Reynolds number in the vicinity of the shock, $\mathrm{Re} \equiv 2\rho_0 c_0 \upsilon_a \tau_{sh}(t) / b$ progressively diminishes. So this is the vicinity of the shock front, where the corrections to the pulse profile due to the dissipation should be first taken into account in the regime characterized by $\varepsilon \mathrm{Re}(t = 0) >> 1$. Thus the common way to describe the pulse evolution in the regime $\varepsilon \mathrm{Re}(t = 0) >> 1$ of interest here is first to analyze the pulse evolution, predicted by Eq. (14) and then to take into account the influence of sound absorption[23], which is the most pronounced in the vicinity of the weak shock fronts.

3.1. Probing transformation of nonlinear acoustic pulse in ideal media before weak shock front formation

In ideal media, characterized by negligible effective viscosity the propagation of the nonlinear acoustic pulses is described by the simple-wave equation (14). The transformation of the pulse profile, predicted by the simple-wave equation (14) is easy to “visualize”.[28-30] In the coordinate system (υ, ξ) all the points $(\upsilon_i(0) = \upsilon(0, \xi_i(0)), \xi_i(0))$ of the initial profile $\upsilon(t = 0, \xi)$ are moving with increasing time horizontally following the law $(\upsilon_i(t) = \upsilon_i(0), \xi_i(t) = \xi_i(0) + \varepsilon\upsilon_i(0)t)$.[28-30] In Fig. 2 (a) we illustrate how this motion of the profile points leads to the formation of the shock front in the initially triangular pulse. The lengths of the horizontal arrows in Fig. 2 (a) increase as $\varepsilon\upsilon_i(0)t$. The letters A, A' and A'' denote in Fig. 2 (a) the positions of the acoustic pulse peak in the initial time moment $t = 0$, in the intermediate time moment $0 < t < t_{sh}$ before the shock front formation and in the moment $t = t_{sh}$ of the front formation, respectively. If the initial full-width-half-maximum (FWHM) length of the triangular pulse is l_a and the amplitude is υ_a, then the time for the shock formation is $t_{sh} = l_a /(\varepsilon\upsilon_a)$. This formula can be used for the estimation of the shock formation time in the pulses of more complicated shape if their profiles can be characterized by only two scales, i.e., l_a and υ_a. Moreover the transformation of the pulse profile presented in Fig. 2 (a) captures the most essential features of the transformation for $0 \le t \le t_{sh}$ of the single-polar pulses of other shapes characterized by only two scales. The analytical description of the pulse profiles in Fig. 2 (a) is

$$\upsilon = \begin{cases} 0, \ if \quad \xi \le -2l_a; \\ \upsilon_a(2l_a + \xi)/(l_a + \varepsilon\upsilon_a t), \ if \quad -2l_a \le \xi \le -l_a + \varepsilon\upsilon_a t; \\ \upsilon_a \xi /(-l_a + \varepsilon\upsilon_a t), \ if \quad -l_a + \varepsilon\upsilon_a t \le \xi \le 0; \\ 0, \ if \quad 0 \le \xi. \end{cases} \tag{15}$$

The substitution of Eq. (15) into Eq. (11) results in

$$\tilde{\eta}_{zz}(t, q = 2k) = -\frac{\upsilon_a}{2ikc_0}\left\{\frac{\sin[k(l_a - \varepsilon\upsilon_a t)]}{k(l_a - \varepsilon\upsilon_a t)} e^{ikl_a} - \frac{\sin[k(l_a + \varepsilon\upsilon_a t)]}{k(l_a + \varepsilon\upsilon_a t)} e^{-ikl_a}\right\} e^{-2ikl_a + ik\varepsilon\upsilon_a t}. \tag{16}$$

For the picosecond laser ultrasonics the most typical and the most important is the situation where the initial length of the photo-generated acoustic pulse is much shorter than the optical wavelength. In this case the first approximation to the precise solution in Eq. (16), which includes the terms of the first order in small parameter $2kl_a << 1$, is

$$\tilde{\eta}_{zz}(t, q = 2k) = -\frac{\upsilon_a l_a}{c_0}(1 - 2ikl_a + 2ik\varepsilon\upsilon_a t/3) \cong -\frac{\upsilon_a l_a}{c_0} e^{-2ikl_a + i\frac{2}{3}k\varepsilon\upsilon_a t} \equiv -\frac{\upsilon_a l_a}{c_0} e^{-2ikl_a + \frac{2ikl_a}{3}\left(\frac{t}{t_{sh}}\right)} . (17)$$

With the accepted precision, the derived solution in Eq. (17) predicts that at the stage of the shock front formation in the profile of the picosecond acoustic pulse the amplitude of the oscillation in transient reflectivity is a constant independent of the material nonlinearity, while the deviation of the oscillation frequency from the Brillouiin frequency is a constant proportional to acoustic nonlinearity ε, acoustic Mach number[23] $M_a \equiv \upsilon_a / c_o$ and the Brillouin frequency itself

$$\omega_{dR/R} - \omega_B \approx \frac{2k}{3}\varepsilon\upsilon_a = \frac{1}{3}\varepsilon M_a \omega_B . \qquad (18)$$

It can be verified that, for the assumed short triangular acoustic pulse, the result in Eq. (18) can be much easier obtained using Eq. (13).

3.2. Picosecond ultrasonic interferometry of acoustic pulse containing weak shock front

In Fig. 2 (b), by the same method of geometrical transformation, we illustrate that after the shock formation, i.e., at times $t > t_{sh}$ the profile of the acoustic pulse predicted by Eq. (14) becomes multi-valued, i.e., non-functional. To avoid this unphysical prediction, the shock front should be introduced in such position $\xi = \xi_{sh}(t)$ that the surface area of the pulse is conserved[23]. This geometrical construction predicts that for $t > t_{sh}$ the length of the strain pulse starts to increase, $l_a(t) = l_a + \xi_{sh}(t)/2$, while the amplitude of the acoustic pulse starts to diminish $\upsilon_a(t) = \upsilon_a l_a / l_a(t)$. The letters A'' and A''' denote in Fig. 2 (b) the positions of the acoustic pulse peak in the moment $t = t_{sh}$ of the front formation and in some moment $t > t_{sh}$ after the shock front formation, respectively. The analytical description of the pulse profile takes the form

$$\upsilon = \upsilon_a(t)\left\langle \left\{ \frac{(\xi + 2l_a)H(\xi + 2l_a) - (\xi - \xi_{sh})H(\xi - \xi_{sh})}{(2l_a + \xi_{sh}(t))} - \frac{1}{2} \right\} \left[-\operatorname{sgn}(\xi - \xi_{sh}(t)) \right] + \frac{1}{2} \right\rangle, \quad (19)$$

where

$$\upsilon_a(t) = \upsilon_a \Big/ \sqrt{1 + \frac{\varepsilon M_a}{2}\left(\frac{t - t_{sh}}{\tau_a}\right)} = \upsilon_a \Big/ \sqrt{1 + \left(\frac{t - t_{sh}}{2t_{sh}}\right)}, \quad (20)$$

$$\xi_{sh}(t) = 2l_a\left[\sqrt{1 + \frac{\varepsilon M_a}{2}\left(\frac{t - t_{sh}}{\tau_a}\right)} - 1\right] = 2l_a\left[\sqrt{1 + \left(\frac{t - t_{sh}}{2t_{sh}}\right)} - 1\right], \quad (21)$$

$H(\xi)$ is the unit step function ($H(\xi < 0) = 0, H(\xi > 0) = 1$) and $\operatorname{sgn}(\xi)$ is the sign function ($\operatorname{sgn}(\xi < 0) = -1, \operatorname{sgn}(\xi > 0) = 1$). It can be checked that the velocity of the shock front propagation in the moving coordinate frame is controlled by the nonlinear acoustic parameter and the amplitude of the acoustic pulse, $\upsilon_{sh}(t) \equiv \partial\xi_{sh}(t)/\partial t = \varepsilon\upsilon_a(t)/2$.

The substitution of Eq. (19) into Eq. (11) results in

$$\tilde{\eta}_{zz}(t, q = 2k) = -\frac{\upsilon_a(t)}{2ikc_0} e^{2ik\xi_{sh}(t)} \left\{ 1 - \frac{1}{4ik\left[l_a + \xi_{sh}(t)/2\right]}\left[1 - e^{-4ik\left[l_a + \xi_{sh}(t)/2\right]}\right] \right\}. \quad (22)$$

At the time scale, when the acoustic pulse, even broadened by the nonlinear processes, is still importantly shorter than the optical wavelength, i.e., $2kl_a(t) = 2k[l_a + \xi_{sh}(t)/2] << 1$, the solution in Eq. (22) can be approximated by the formula

$$\tilde{\eta}_{zz}(t, q = 2k) = -\frac{\upsilon_a l_a}{c_0} e^{-\frac{4}{3}ikl_a + i\frac{4}{3}k\xi_{sh}(t)}, \quad (23)$$

which predicts that after the shock formation the difference between the detected frequency and the Brillouin frequency starts to diminish

$$\omega_{dR/R}-\omega_B \approx \frac{4}{3}k\upsilon_{sh}(t)=\frac{1}{3}\varepsilon M_a(t)\omega_B\,. \tag{24}$$

In Eq. (24) $M_a(t)$ denotes the current acoustic Mach number, $M_a(t)=M_a\Big/\sqrt{1+\frac{\varepsilon M_a}{2}\left(\frac{t-t_{sh}}{\tau_a}\right)}=M_a\Big/\sqrt{1+\left(\frac{t-t_{sh}}{2t_{sh}}\right)}$. The condition $2kl_a(t)<<1$, required for the validity of Eq. (23) and Eq. (24), can be rewritten under the assumption $2kl_a(t=0)<<1$ as $t-t_{sh}<<2[2kl_a]^{-2}t_{sh}\equiv t_{sh}^{(1)}$. Because of $t_{sh}^{(1)}>>t_{sh}$ it can be concluded that the considered approximation could be valid at time scale significantly exceeding the characteristic nonlinear time t_{sh} of the shock front formation.

With the increasing time, due to the nonlinear broadening of the acoustic pulse, the role of the second term in the figure brackets in Eq. (22), which describes the light scattering by the trailing edge of the strain pulse (see Fig. 2 (b)), progressively diminishes. This term is comparable with the first term only if $2kl_a(t)\le 1$. At larger times the solution in Eq. (22) predicts that the dominant scattering of the probe light is by the leading shock front of the acoustic pulse, where the strain gradients are much higher than in the trailing front

$$\tilde{\eta}_{zz}(t,q=2k)=-\frac{\upsilon_a(t)}{2ikc_0}e^{2ik\xi_{sh}(t)}=\frac{\upsilon_a(t)}{2kc_0}e^{2ik\xi_{sh}(t)+i\pi/2}. \tag{25}$$

In this regime the amplitude of the oscillation in transient reflectivity diminishes with time following the fall in the pulse amplitude, described by Eq. (20), while the oscillation frequency is a measure of the shock front velocity. In fact, it follows from Eq. (25) that $\omega_{dR/R}-\omega_B\approx 2k\upsilon_{sh}(t)=(\varepsilon M_a(t)/2)\omega_B$. So, if to the experimental measurement of frequency we associate the measurement of the velocity through the relation $\omega_{dR/R}=2kc_{dR/R}$ similar to $\omega_B=2kc_0$, which holds for the Brillouin frequency, then in the considered regime the measured velocity $c_{dR/R}$ is $c_{dR/R}=c_0+\upsilon_{sh}(t)\equiv c_{sh}$. Thus we are measuring the velocity c_{sh} of the weak shock front in laboratory, i.e., immobile, coordinate frame. The velocity c_{sh} of the compression shock, i.e., of the one with $\upsilon_a(t) > 0, \eta_{zz} < 0$, in medium with positive parameter of acoustic nonlinearity ($\varepsilon > 0$), is supersonic ($c_{sh} > c_0$).

The regime of monitoring of the shock front velocity by time-resolved Brillouin scattering can be understood more generally, by transforming Eq. (11) through the integration by parts, into

$$\tilde{\eta}_{zz}(t, q = 2k) = \frac{1}{2ikc_0} \int_{-\infty}^{\infty} \frac{\partial \upsilon(t,\xi)}{\partial \xi} e^{i2k\xi} d\xi . \qquad (26)$$

The solution in Eq. (26) has a clear physical sense that scattering of light is caused by strain gradients and not by the homogeneous strain. Homogeneous strain distribution can not contain the spatial Fourier component at $q = 2k \neq 0$. When the nonlinear acoustic processes progressively shorten one front of the strain pulse and broaden the other one, high spatial Fourier frequencies are progressively more and more spatially localized in the narrower front. Finally, when the broader front of the acoustic pulse provides negligible contribution to Eq. (26), because of low spatial gradients of the strain in this front, then time-resolved reflectivity measurements monitor the evolution of the shorter front, i.e., of the shock front, only. The formal substitution in Eq. (26) of the delta-localized shock front, i.e., $\partial \upsilon(t,\xi) / \partial \xi \approx -\upsilon_a(t)\delta(\xi - \xi_{sh}(t))$, immediately reproduces differently derived solution in Eq. (25).

We can conclude, that time-resolved Brillouin scattering always selects from the acoustic wave profile the spatial Fourier component with $q = 2k$, however, in the case of the pronounced nonlinear transformation of the coherent acoustic pulse profile accompanied by the shock front formation, this particular component (Brillouin component) is spatially localized in the shock front and moves due to nonlinear processes not with the velocity of the linear acoustic waves c_0 but with the velocity of the shock front $c_{sh} = c_0 + \upsilon_{sh}(t)$. Correspondingly, the measured frequency of the oscillation in transient reflectivity differs from the Brillouin frequency that should be observed in the linear regime of the coherent acoustic pulse propagation.

It is worth repeating here that the formation of the weak shock front and its subsequent decay in amplitude and deceleration in propagation velocity are all the results of nonlinear multi-scattering acoustic processes involving all the spectral components of the wide-frequency-band picosecond acoustic pulse. They all depend on the particular initial profile of the laser-generated picosecond strain pulse. The deviation of $\omega_{dR/R}$ from ω_B is not just the result of the nonlinear self-action of the spectral component with the frequency equal to ω_B. It is well known in nonlinear acoustics[23] that in the initially sinusoidal acoustic wave of finite amplitude, in the case of elastic quadratic acoustic nonlinearity accounted by Eqs. (10) and (14), the weak shock fronts are formed inside each spatial period of the wave, but they all propagate at the velocity of the linear sound c_0, i.e., they are immobile in the moving sonic coordinate frame. So if a purely sinusoidal strain wave at frequency ω_B could be laser-generated (for example, in the process of the stimulated Brillouin scattering of the pump laser radiation[28]) its nonlinear transformation in the media with quadratic elastic nonlinearity would not result in the shift of $\omega_{dR/R}$ relative to ω_B.

The solution in Eq. (22) describes the transition from monitoring of the both fronts of the acoustic pulse (Eq. (23)) to monitoring of the shock front only (Eq. (24)). Introducing the compact notations $4k[l_a + \xi_{sh}(t)/2] = 4kl_a(t) = 8\pi l_a(t)/\lambda \equiv \Lambda(t)$ for the normalized length of the strain pulse and $\sin c(x) \equiv \sin(x)/x$ for the *sinc* function, we rewrite the solution in Eq. (22) as

$$\tilde{\eta}_{zz}(t, q = 2k) = -\frac{\upsilon_a(t)}{2kc_0}\sqrt{1 - 2\sin c(\Lambda) + \sin c^2(\Lambda/2)}\, e^{2ik\xi_{sh}(t) - i\arctan\left[\frac{1-\sin c(\Lambda)}{(\Lambda/2)\sin c^2(\Lambda/2)}\right]}. \qquad (27)$$

The square root in Eq. (27), $\Xi(t) \equiv \sqrt{1 - 2\sin c(\Lambda) + \sin c^2(\Lambda/2)}$, describes transitional modulation of the Brillouin signal amplitude (Fig. 3 (a)), which is superimposed on the asymptotic dependence $A_\eta(t) \propto \upsilon_a(t)$. The dependence on $\Lambda(t)$ of the phase of the signal in Eq. (27) results in transitional modulation of the frequency of the transient reflectivity oscillation, proportionally to $\Theta(\Lambda) \equiv \dfrac{1 - \sin c(\Lambda)}{1 - 2\sin c(\Lambda) + \sin c^2(\Lambda/2)}$ (Fig. 3 (b)), which is superimposed on the asymptotic dependence $\omega_{dR/R} \propto \upsilon_{sh}(t)\omega_B \propto \varepsilon M_a(t)\omega_B$:

$$\omega_{dR/R} - \omega_B = 2k\upsilon_{sh}(t)\left[\frac{1 - \sin c(\Lambda)}{1 - 2\sin c(\Lambda) + \sin c^2(\Lambda/2)}\right] = \frac{\varepsilon M_a(t)}{2}\left[\frac{1 - \sin c(\Lambda)}{1 - 2\sin c(\Lambda) + \sin c^2(\Lambda/2)}\right]\omega_B .$$

(28)

The transitional modulations are due to the interference between the light waves scattered by the leading and trailing edges of the strain pulse. They disappear when the scattering of light by one of the fronts becomes negligible. In accordance with the analysis presented above the transitional regime described by Eq. (27) takes place when the inequality $2kl_a(t) \leq 1$ holds. This condition can be rewritten as $t - t_{sh} \leq 2[2kl_a]^{-2} t_{sh} \equiv t_{sh}^{(1)}$, demonstrating that, because of the strong inequality $2kl_a << 1$, the monitoring of the motion of the shock front only could be possible only after time delay which is importantly longer than the characteristic nonlinear time t_{sh}.

3.3. Influence on the time-resolved Brillouin scattering signals of finite shock front duration.

Infinitely short shock fronts of the nonlinear acoustic pulses in Fig. 2 (a) and (b) are just the first approximation, which is provided by the precise solution of the simple-wave equation (Eq. (14)) to the solutions of the Burgers equation (Eq. (10)) in the case, where the initial pulse is characterized by the inequality $\varepsilon \operatorname{Re}(t=0) >> 1$. In this regime in the next approximation the finite duration of the shock front could be taken into account by replacing in the solution (19) the multiplier $\operatorname{sgn}(\xi - \xi_{sh}(t))$ by $\tanh\left[\frac{\xi - \xi_{sh}(t)}{\Delta\xi_{sh}(t)}\right]$, where *tanh* denotes the hyperbolic tangent function and the width of the shock front $\Delta\xi_{sh}(t)$ depends on the shock amplitude $\Delta\xi_{sh}(t) \equiv c_0 \tau_{sh} = 2b/\left[\varepsilon\rho_0 \upsilon_a(t)\right] = \left[4/(\varepsilon \operatorname{Re})\right] l_a \sqrt{1 + \left(\frac{t - t_{sh}}{2t_{sh}}\right)}$.[23] It can be verified that, with thus defined shock front width, the local acoustic Reynolds number in the shock front region $\operatorname{Re} \equiv 2\rho_0 c_0 \upsilon_a \tau_{sh}(t)/b$ is equal to $4/\varepsilon$. Consequently inside the shock the estimate $\varepsilon \operatorname{Re} \propto 1$ is valid and the processes of the linear high frequency absorption causing front broadening are as important as the nonlinear processes leading to front shortening. Front broadens following the diminishing of its amplitude, $\Delta\xi_{sh}(t) \propto 1/\upsilon_a(t)$. The solution, which is obtained in this approximation, seems to be accurate enough as far as the shock front retains its physical sense, i.e. as far as it is sufficiently shorter than the total length of the acoustic pulse,

$$\Delta\xi_{sh}(t)=\left(\frac{4}{\varepsilon\,\mathrm{Re}}\right)l_a\sqrt{1+\left(\frac{t-t_{sh}}{2t_{sh}}\right)}<<l_a(t)=l_a+\frac{\xi_{sh}(t)}{2}=l_a\sqrt{1+\left(\frac{t-t_{sh}}{2t_{sh}}\right)}. \qquad (29)$$

In the regime $\varepsilon\,\mathrm{Re}>>1$ this inequality reasonably holds until complete absorption of the acoustic pulse. However it is known[23] that thus derived solutions can not be used till $t=\infty$, because in the adopted approximation the next order effect, consisting in the diminishing of the pulse amplitude $\upsilon_a(t)$, when the shock front of the finite duration replaces the infinitely short shock front, is not taken into account. This, additional to one described by Eq. (20), diminishing of $\upsilon_a(t)$, leads to additional broadening of the shock front due to the relation $\Delta\xi_{sh}(t)\propto 1/\upsilon_a(t)$, forming the inverse loop. The described slowly accumulating effect is known to lead at long time scale to the symmetrical single polar pulses with equal duration of the leading and the trailing fronts, as we will demonstrate a bit later through the analysis of a particular precise solution of the Burgers equation. Here we note that the conditions of the confident validity of the method of the shock front installation can be found, by requesting that the installation of the shock front $\Delta\xi_{sh}(t)\propto 1/\upsilon_a(t)$ in the pulse profile leads to the negligible changes in the pulse amplitude even if the increase in the pulse width $l_a(t)$ is neglected, i.e., if the front of the increasing width is installed in the fixed initial pulse profile. This transforms the validity condition in Eq. (29) into more restrictive one

$$\Delta\xi_{sh}(t)=\left(\frac{4}{\varepsilon\,\mathrm{Re}}\right)l_a\sqrt{1+\left(\frac{t-t_{sh}}{2t_{sh}}\right)}<<l_a(0)\equiv l_a, \qquad (30)$$

which even for $\varepsilon\,\mathrm{Re}>>1$ provides the upper time limit for validity of the solutions $t-t_{sh}<<2(\varepsilon\,\mathrm{Re}/4)^2 t_{sh}\equiv t_{sh}^{(2)}$. We conclude that, because of the inequality $\varepsilon\,\mathrm{Re}>>1$, the obtained solutions are valid at the time scale importantly larger than the characteristic nonlinear scale t_{sh} of the pulse broadening due to nonlinearity. If the inequality $(2kl_a)^{-2}<(\varepsilon\,\mathrm{Re}/4)^2$ holds, then $t_{sh}^{(1)}<t_{sh}^{(2)}$ and in the time interval $t_{sh}^{(1)}\le t\le t_{sh}^{(2)}$ the influence of the front broadening on the transient reflectivity signal takes place when the influence of the light scattered by the trailing front of the pulse is negligible.

To capture the essential influence of the shock front broadening on the transient reflectivity signal, but avoiding cumbersome formulas, we approximate the tanh-type shock front by the linear shock front

$$-\tanh\left[\frac{\xi-\xi_{sh}(t)}{\Delta\xi_{sh}(t)}\right]\Rightarrow\begin{cases}1,\ if\quad \xi\le\xi_{sh}(t)-\Delta\xi_{sh}(t);\\ -\xi/\Delta\xi_{sh}(t)\ \ if\quad \xi_{sh}(t)-\Delta\xi_{sh}(t)\le\xi\le\xi_{sh}(t)+\Delta\xi_{sh}(t);\\ -1,\ if\quad \xi\ge\xi_{sh}(t)+\Delta\xi_{sh}(t).\end{cases}$$

Correspondingly, the spatial derivative of the pulse profile inside the shock front, *i.e.*, when $\xi_{sh}(t)-\Delta\xi_{sh}(t)\le\xi\le\xi_{sh}(t)+\Delta\xi_{sh}(t)$, is given by $\partial\upsilon(t,\xi)/\partial\xi\approx-\left[\upsilon_a(t)/(2\Delta\xi_{sh}(t)\right]$. Then the evaluation of Eq. (26) leads to

$$\tilde{\eta}_{zz}(t,q=2k)=-\frac{\upsilon_a(t)}{2ikc_0}\left[\frac{\sin(2k\Delta\xi_{sh})}{2k\Delta\xi_{sh}}\right]e^{2ik\xi_{sh}(t)}. \tag{31}$$

The solution in Eq. (31) indicates that continuous broadening of the shock front is the source of the modulation of the transient reflectivity amplitude, which is superimposed on the asymptotic dependence $A_\eta(t)\propto\upsilon_a(t)$. Note, that because of the inequality (29), the solution in Eq. (31) indicates that this modulation is activated only after the disappearance of the modulation caused by the light reflection from the long trailing edge of the nonlinear acoustic pulse. It is important that, in the frame of the accepted approximations, the absorption causes shock front broadening but does not induce shock front displacement relative to $\xi=\xi_{sh}(t)$, which was predicted earlier in the absence of absorption. This results in the absence of the modification of the phase of the signal in Eq. (31) except at the time instances defined by the solutions of $2k\Delta\xi_{sh}(t)=\pi n$, where $n=1,2,...$ is the integer number. At these time moments the phase of the Brillouin oscillation abruptly changes by π. If the phase is appropriately unrapped, then these changes do not result in any modulation of the oscillation frequency additional to the asymptotic dependence $\omega_{dR/R}-\omega_B\propto\upsilon_{sh}(t)\omega_B\propto\varepsilon M_a(t)\omega_B$ revealed earlier.

3.4. Influence on the signals of transient broadening of the initially laser-generated weak shock fronts

It is important to note that the conditions of the validity of above derived description of the time-resolved light scattering by the coherent acoustic pulses could be broader than given by the inequality $\varepsilon \,\mathrm{Re}(t=0) >> 1$. In fact, the description of the finite width of the shock front $\Delta\xi_{sh}(t) \equiv c_0\tau_{sh} = 2b/[\varepsilon\rho_0\upsilon_a(t)] = [4/(\varepsilon\,\mathrm{Re})]l_a\sqrt{1+\left(\frac{t-t_{sh}}{2t_{sh}}\right)}$, accepted above, is suggested by the stationary shock fronts predicted by existing analytical solutions of the Burgers equation. Stationary shock fronts are the time-independent smoothed step-like wave profiles moving with constant velocity, different from the velocity c_0 of the linear sound.[23] So the above proposed solutions had not taken into account that in the transient problems of acoustic pulse propagation it could take finite time to smooth the initially step-like profile. Let us illustrate this statement by a typical example from picosecond laser ultrasonics. In picosecond laser ultrasonics in many cases the initially photo-generated, i.e., just after the thermalization in the material of the energy absorbed from the femtosecond laser pulse, single polar acoustic strain pulse has a highly asymmetric shape which is much closer to that described by Eq. (15) and in Fig. 2 at $t=t_{sh}$ than at $t=0$. In other words the initial pulse and its evolution should be rather described not by Eq. (15) and Eq. (19) but just by Eq. (19) with the shift of the initial time moment, i.e., $t-t_{sh}\Rightarrow t$. In this description the characteristic width of the initial pulse is approximately equal to the initial length of trailing front. In the case of the emission of the acoustic pulses in the transparent medium from the light absorbing medium this characteristic length l_a could be controlled by the length of optical energy transfer to the material atoms in the opaque medium or by the thickness of the opaque medium, for example. The length of the leading front could be controlled by the distance of acoustic wave propagation either during the femtosecond laser action or during the time of the absorbed energy transfer to the material atoms, or by the characteristic roughness of the interface between opaque and transparent media, for example. The initial width of the leading front is negligible in comparison with the width of the trailing front. So we can try to treat it as shock front of the initial amplitude υ_a. However, it would be incorrect to replace the infinitely thin shock front in Eq. (19) by the front of the finite width $\Delta\xi_{sh}(t) \equiv c_0\tau_{sh} = 2b/[\varepsilon\rho_0\upsilon_a(t)] = [4/(\varepsilon\,\mathrm{Re})]l_a\sqrt{1+t/(2t_{sh})}$ immediately, that is starting from $t=0$. This follows from the precise solution of the linearized Burgers equation, i.e., of the equation $\frac{\partial\upsilon}{\partial t}-\frac{b}{2\rho_0}\frac{\partial^2\upsilon}{\partial\zeta^2}=0$, with the initial condition $\upsilon(t=0,\xi)=\upsilon_a[1-\mathrm{sgn}(\xi)]$. This precise solution reads $\upsilon(t=0,\xi)=\upsilon_a\left[1-erf(\xi/\sqrt{2bt/\rho_0})\right]$ and predicts that the broadening of the front width $\Delta\xi_{abs}$ caused by the high frequency absorption in the absence of the nonlinear processes follows the diffusion law $\Delta\xi_{abs}(t)=\sqrt{2bt/\rho_0}$. This could have been expected because the linearized Burgers equation is the linear diffusion-type equation. We can conclude that, if the nonlinearity is taken into account, the duration of the shock front could be estimated by the earlier proposed $\Delta\xi_{sh}(t)$ only at the time scales when $\Delta\xi_{sh}(t)\le\Delta\xi_{abs}(t)$. This inequality reduces to

$$t \ge 2t_{sh}/(\varepsilon\,\mathrm{Re}/2-1)\equiv t_\infty . \qquad (32)$$

When $\varepsilon\,\mathrm{Re}>>1$, the inequality (32) is satisfied starting from the critical time $t_\infty << t_{sh}$. This confirms the validity of the solutions, that were derived above (for $\varepsilon\,\mathrm{Re}>>1$ at the time scales $t_{sh}\le t\le 2(\varepsilon\,\mathrm{Re}/4)^2 t_{sh}$ of interest, when the shock front displacement in the sonic coordinate frame could be appreciated) through the installation of the stationary front of the width $\Delta\xi_{sh}(t)\le\Delta\xi_{abs}(t)$. Note, that for the acoustic pulses containing initially the shock front, the characteristic time $t_{sh}=l_a/(\varepsilon\upsilon_a)$ should be understood not as the time of shock front formation, but just as the characteristic time of the possible broadening of the initial acoustic pulse due to the nonlinearity. In accordance with $l_a(t)=l_a\sqrt{1+t/(2t_{sh})}$ at $t=6t_{sh}$ the length of the initial triangular pulse could be doubled.

When the inequality in Eq. (32) is not satisfied, then the duration of the shock front to be installed in the solution Eq. (19) should be $\Delta\xi_{abs}(t)=\sqrt{2bt/\rho_0}$, and the condition of the negligible influence of the shock front broadening on the front amplitude results in the equality $\sqrt{2bt/\rho_0}<<l_a$. This inequality can hold even for the acoustic waves of low amplitude, when $t<<t_{sh}$ in the experimental observation time window, if $t<<l_a^2/(2b/\rho_0)\equiv t_{abs}^{l_a}$. At this time scale the initial shock front in the laser-generated acoustic strain pulse is well-defined and even slow shock front motion in the sonic coordinate frame could be still detected as it is described by Eq. (27) and Eq. (28), if the measurement of $\omega_{dR/R}$ are possible with the necessary precision. Note, that $(\omega_{dR/R}-\omega_B)/\omega_B\propto\varepsilon M_a(t)\propto\upsilon_{sh}(t)/c_0$ could be very small in this quasi-linear regime. Consequently, the monitoring of the shock front motion could be possible due to the creation of weak shock front by pump laser action and not in the process of the acoustic pulse propagation.

The above presented theoretical analysis demonstrates that through the measurements of the frequency $\omega_{dR/R}$ of the time-resolved reflectivity signal there is an access to the measurements of the parameter of acoustic nonlinearity, because the nonlinearity is responsible for the difference between $\omega_{dR/R}$ and ω_B. Speaking differently $\omega_{dR/R} - \omega_B \neq 0$ only if $\varepsilon \neq 0$. Although the information on ε could be formally extracted from the experimental data in any regime of the nonlinear propagation of the coherent acoustic pulse, the most straightforward analysis of the experimental data can be achieved in the regime $\varepsilon \mathrm{Re} >> 1$ when in the time interval $2(2kl_a)^{-2} t_{sh} \leq t \leq 2(\varepsilon \mathrm{Re}/4)^2 t_{sh}$ the transient reflectivity oscillation is caused by light scattering from a single well-defined moving shock front in the profile of the coherent acoustic pulse. In this regime $\omega_{dR/R} - \omega_B \cong 2k\upsilon_{sh}(t)$. For $2kl_a(0) << 1$ in this regime the relations $t >> t_{sh}$ and $\sqrt{1+(t-t_{sh})/(2t_{sh})} \approx \sqrt{t/2t_{sh}}$ hold, resulting in a particularly simple prediction for the time evolution of the measured frequency $\omega_{dR/R} - \omega_B \cong \sqrt{\frac{\varepsilon\upsilon_a\tau_a}{2c_0 t}}\omega_B \propto \sqrt{\varepsilon S/t} \propto 1/\sqrt{t}$. Consequently, through the fitting of the experimentally measured $[\omega_{dR/R}(t) - \omega_B]/\omega_B$ only the product $\varepsilon\upsilon_a\tau_a = \varepsilon\upsilon_a l_a / c_0 \equiv \varepsilon S$ can be measured. To extract the nonlinear acoustic parameter it is additionally necessary either to measure $\upsilon_a\tau_a$ in some other experiments or to estimate $\upsilon_a\tau_a$ theoretically.

The dependence of the predicted $\omega_{dR/R} - \omega_B$ in the considered regime only on the initial surface area of the acoustic pulse $S \equiv \upsilon_a l_a = \upsilon_a\tau_a c_0$, but not on υ_a and τ_a separately, indicates that the information on the initial pulse shape has disappeared at the considered long time delays. From this point of view fitting of the experimental data at shorter time scales, although more complicated, could be more fruitful. For example, in the theoretical prediction in Eq. (27) the variations of phase in time depend not only on the displacement of the shock front $\xi_{sh}(t)$ but also on the initial pulse length (duration) through the dependence on the non-dimensional parameter $\Lambda(t) = 8\pi k[l_a + \xi_{sh}(t)/2] = 8\pi k[c_0\tau_a + \xi_{sh}(t)/2]$ (see Fig. 3). Correspondingly, $\omega_{dR/R} - \omega_B$ in Eq. (28) depends on the weak, i.e., acoustic, shock front velocity $\upsilon_{sh}(t) = \frac{\varepsilon\upsilon_a(t)}{2} = \frac{\varepsilon\upsilon_a}{2}\sqrt{\frac{1}{2}\left(1+\frac{\varepsilon\upsilon_a t}{2c_0\tau_a}\right)}$ and $\Lambda(t) = 8\pi k l_a(t) = 8\pi k c_0\tau_a\sqrt{\frac{1}{2}\left(1+\frac{\varepsilon\upsilon_a t}{2c_0\tau_a}\right)}$, and, thus, it is the function of two independent parameters $\varepsilon\upsilon_a$ and τ_a. Both parameters can be determined by fitting the experimental data. Then to extract the parameter of the acoustic nonlinearity it is necessary to determine through additional experiments or estimate theoretically only the amplitude υ_a of the particle velocity in the photo-generated acoustic pulse. This situation is similar to one existing in the physics of strong, i.e., non-acoustic, shock waves, where in order to determine the equation of state at high pressures in addition to the measurements of the strong shock front velocity it is necessary to measure independently the flow velocity, i.e., the velocity of the particles, at least at one particular coordinate or in one particular moment of time.[31-36]

3.5. Brillouin scattering caused by multi-phase nonlinear acoustic pulses in the regime of arbitrary Reynolds numbers

The most complicated for the approximate analytical description is the propagation of the acoustic pulses characterized by the condition $\varepsilon \mathrm{Re} \propto 1$, when the roles of the nonlinear and the dissipation effects in the Burgers equation (Eq. (10)) are comparable from the beginning. In this case there is in principle formal opportunity to describe the evolution of the pulse profile precisely, however thus obtainable solutions in most of the cases are too cumbersome to provide insight in the physics of the processes of interest[23]. To obtain the analytical solution of Eq. (10) it is first convenient to rewrite it by introducing non-dimensional slow time $\vartheta = t / t_{sh} = \varepsilon \upsilon_a t / l_a$, non-dimensional profile coordinate $\sigma = \xi / l_a$, non-dimensional particle velocity $V = \upsilon / \upsilon_a$ and the compact notation $1/(\varepsilon \mathrm{Re}) \equiv \Gamma / 4$. The equation takes the form

$$\frac{\partial V}{\partial \vartheta} + V \frac{\partial V}{\partial \sigma} - \frac{\Gamma}{4} \frac{\partial^2 V}{\partial \sigma^2} = 0, \qquad (33)$$

which confirms the crucial role played by the parameter $\varepsilon \mathrm{Re}$, as it had been discussed earlier. The nonlinear transformation of the function, the so-called Hopf–Cole transformation,[23]

$$V = -\frac{\Gamma}{2} \frac{\partial \ln U}{\partial \sigma} = -\left(\frac{\Gamma}{2}\right) \frac{1}{U} \frac{\partial U}{\partial \sigma}, \qquad (34)$$

transforms the nonlinear Eq. (32) in linear diffusion equation

$$\frac{\partial U}{\partial \vartheta}-\frac{\Gamma}{4}\frac{\partial^2 U}{\partial \sigma^2}=0\,. \tag{35}$$

The diffusion equation has formal analytical solutions in the integral form, for arbitrary initial conditions $U(0,\sigma)$

$$U(\vartheta,\sigma)=\frac{1}{\sqrt{\pi\Gamma\vartheta}}\int_{-\infty}^{\infty}e^{-\left(\frac{\sigma-\sigma'}{\sqrt{\Gamma\vartheta}}\right)^2}U(0,\sigma')d\sigma'\equiv\frac{1}{\sqrt{\pi}a}\int_{-\infty}^{\infty}e^{-\left(\frac{\sigma-\sigma'}{a}\right)^2}U(0,\sigma')d\sigma'\,. \tag{36}$$

Here we have introduced the compact notation $a(\vartheta)\equiv\sqrt{\Gamma\vartheta}$. The solution for the spatial derivative can be presented, using Eq. (34), in the convenient form

$$\frac{\partial U(\vartheta,\sigma)}{\partial\sigma}=\frac{1}{\sqrt{\pi}a}\int_{-\infty}^{\infty}e^{-\left(\frac{\sigma-\sigma'}{a}\right)^2}\frac{\partial U(0,\sigma')}{\partial\sigma'}d\sigma'=\frac{-1}{\sqrt{\pi}a}\left(\frac{2}{\Gamma}\right)\int_{-\infty}^{\infty}e^{-\left(\frac{\sigma-\sigma'}{a}\right)^2}U(0,\sigma')V(0,\sigma')d\sigma'. \tag{37}$$

The initial distribution $U(0,\sigma)$ can be obtained from the initial conditions $V(0,\sigma)$ by using the inversion of Eq. (34), i.e.,

$$U(\vartheta,\sigma)=\exp\left[-\frac{2}{\Gamma}\int^{\sigma}V(\vartheta,\sigma')d\sigma'\right]=\overline{C}\exp\left[-\frac{2}{\Gamma}\int_{\infty}^{\sigma}V(\vartheta,\sigma')d\sigma'\right]\equiv\overline{C}\exp\left[\frac{2}{\Gamma}S(\vartheta,\sigma)\right]. \tag{38}$$

Here $\overline{C}$ is the integration constant and the function $S(\sigma)$ has the sense of the surface area of the acoustic pulse starting from the co-ordinate σ up to the pulse beginning at $+\infty$, i.e., to the right of the co-ordinate σ. The more independent parameters are necessary for the description of the initial acoustic pulse profile $V(0,\sigma)$, the less are chances to get the solution of Eq. (35) not in the form of the integrals or infinite sums, but in functional form on the basis of common and not “exotic” special functions.

An important in picosecond laser ultrasonics class of the initial strain profiles corresponds to the generation of the acoustic pulses in the thin light absorbing films, when the laser-induced heating of the film material can be considered as spatially homogeneous and instantaneous, while the cooling can be considered as infinitely long. What is emitted from the film in the surrounding material is the sequence of the rectangular strain pulses with their amplitudes and signs controlled by the reflection coefficients of acoustic waves at the interfaces between the film and the surrounding material. The duration of each pulse in the sequence is equal to the time of sound propagation across the film $\tau_a = H_f / c_f$, where H_f is the film thickness and c_f is the sound velocity in the film. The typical particle velocity profile launched outside the film is presented qualitatively in Fig. 4. Although the positions of the successive fronts ξ_i (i=1, 2, 3, ...) in the initial profile in Fig. 4 are equidistant, separated by the same distance $l_a = c\tau_a = (c/c_f)H_f$, we have not included this fact in the notations in Fig. 4 for the generality. When the normalized coordinate $\sigma = \xi / l_a$, the normalized particle velocity $V = \upsilon / \upsilon_a$ and the normalized time by $\vartheta = t / t_{sh} = t /[l_a /(\varepsilon\upsilon_a)]$ are introduced, the normalized profile in Fig. 4 provides the initial condition for Eq. (33). Then the initial condition for Eq. (35) can be obtained, using Eq. (38), in the form

$$U(0,\sigma_{n+1} < \sigma < \sigma_n) \equiv U_n(0,\sigma) = \overline{C}\,\exp\{(2/\Gamma)[S_n + V_n(\sigma_n - \sigma)]\}, \tag{39}$$

where $S_n \equiv S(0,\sigma_n) = \sum_{j=0}^{n} V_{j-1}(\sigma_{j-1} - \sigma_j)$ is the surface area of the pulse between $\sigma = \sigma_n$ and $\sigma = \infty \equiv \sigma_0$ and $V(\sigma = \infty) \equiv V_0 = 0$. With this boundary condition, using Eq. (36) and Eq. (37), we derive

$$\begin{aligned} U(\vartheta,\sigma) &= \frac{1}{2}\sum_{n=0}^{\infty} U_n(0,\sigma) e^{(aV_n/\Gamma)^2}\left\{ erf\left[\frac{\sigma_n - \sigma + a^2V_n/\Gamma}{a}\right] - erf\left[\frac{\sigma_{n+1} - \sigma + a^2V_n/\Gamma}{a}\right]\right\}, \\ \frac{\partial U(\vartheta,\sigma)}{\partial\sigma} &= -\frac{1}{\Gamma}\sum_{n=0}^{\infty} V_n U_n(0,\sigma) e^{(aV_n/\Gamma)^2}\left\{ erf\left[\frac{\sigma_n - \sigma + a^2V_n/\Gamma}{a}\right] - erf\left[\frac{\sigma_{n+1} - \sigma + a^2V_n/\Gamma}{a}\right]\right\}. \end{aligned} \tag{40}$$

Here $U_n(0,\sigma)$ is defined by Eq. (39). Substitution of Eq. (40) into Eq. (34) provides analytical description of the acoustic propagation for arbitrary magnitude of the parameter $\varepsilon\,\mathrm{Re} \equiv 4/\Gamma$. However the Fourier transform of the predicted signal, when it is substituted in Eq. (11) for the evaluation of the oscillations in transient optical reflectivity, has to be done numerically. As a simplest example we present the solution in Eq. (40) for the initial single rectangular pulse localized between $\sigma_2 = -1/2$ and $\sigma_1 = 1/2$ and characterized by a single non-zero amplitude $V_1 = 1$

$$U(\vartheta,\sigma)=\frac{\overline{C}}{2}\left\{1-erf\left(\frac{1/2-\sigma}{a}\right)+e^{2(1/2-\sigma)/\Gamma}e^{(aV_n/\Gamma)^2}\left[erf\left(\frac{1/2-\sigma+a^2V_n/\Gamma}{a}\right)\right.\right.$$
$$\left.\left.-erf\left(\frac{-1/2-\sigma+a^2V_n/\Gamma}{a}\right)\right]+e^{2/\Gamma}\left[erf\left(\frac{-1/2-\sigma}{a}\right)+1\right]\right\}, \qquad (41)$$
$$\frac{\partial U(\vartheta,\sigma)}{\partial\sigma}=-\frac{\overline{C}}{\Gamma}e^{2(1/2-\sigma)/\Gamma}e^{(aV_n/\Gamma)^2}\left[erf\left(\frac{1/2-\sigma+a^2V_n/\Gamma}{a}\right)-erf\left(\frac{-1/2-\sigma+a^2V_n/\Gamma}{a}\right)\right].$$

Using either the solution in Eq. (41) or general formulas in Eq. (36) and Eq. (37) in the case of the initially symmetrical pulse, it is straightforward do verify that the asymmetry in the pulse profile, which is introduced by the nonlinearity when the pulse starts to propagate, inevitably disappears at longer time scales. For example, the general solution in Eq. (37) for the derivative takes, in the case of the initial rectangular pulse at the time scales $a(\vartheta)\geq 1$, the following form

$$\frac{\partial U(\vartheta,\sigma)}{\partial\sigma}=\frac{-1}{\sqrt{\pi}a}\left(\frac{2}{\Gamma}\right)\int_{-1/2}^{1/2}e^{-\left(\frac{\sigma-\sigma'}{a}\right)^2}U(0,\sigma')d\sigma'\cong\frac{-1}{\sqrt{\pi}a}\left(\frac{2}{\Gamma}\right)e^{-\left(\frac{\sigma}{a}\right)^2}\int_{-1/2}^{1/2}\left[1-\left(\frac{\sigma'}{a}\right)^2+2\left(\frac{\sigma}{a}\right)\sigma'\right]e^{\frac{2}{\Gamma}\left(\frac{1}{2}-\sigma'\right)}d\sigma'.$$

The integration leads to the following ratio P between the asymmetric, proportional to σ/a, and symmetric, independent of the co-ordinate, contributions to the derivative: $\mathrm{P}\approx-\left[\tanh^{-1}(1/\Gamma)-\Gamma\right]\left[\sigma/a(\vartheta)\right]$. Thus in the limit of strong absorption, when $\varepsilon\,\mathrm{Re}<<1$, while $\Gamma>>1$, we estimate $\mathrm{P}\approx-(1/3)(1/\Gamma)\left[\sigma/a(\vartheta)\right]$. This indicates the low level of asymmetry as expected. However even in the regime of the initially strong nonlinearity when $\varepsilon\,\mathrm{Re}>>1$, while $\Gamma<<1$, we estimate $\mathrm{P}\approx-\left[\sigma/a(\vartheta)\right]$. This indicates the diminishing of pulse asymmetry with increasing time when $a(\vartheta)\geq 1$ and that the asymptotic of the evaluated derivative will be the Gaussian profile. At the same time the asymptotic form of the profile $U(\vartheta,\sigma)$, which follows from Eq. (41) when $a(\vartheta)>>1$, is $U(\vartheta,\sigma)\cong C\left[1+\exp(2/\Gamma)\right]$, that is co-ordinate independent. Thus in accordance with Eq. (34) the asymptotic form of the profile of the acoustic pulse $V(\vartheta\to\infty,\sigma)$ is a Gaussian, confirming the statement formulated in Section 5.1 on the disappearance of the acoustic pulse asymmetry at sufficiently long time scales[23].

The importance of the solution in Eqs. (34) and (40) is in the opportunity, by applying in Eq. (11) the numerical Fourier transform, to derive the predictions for the evolution of the amplitude and the phase of the Brillouin oscillation in the most complicated regime characterized by

$\varepsilon \mathrm{Re} \propto 1$, where the asymptotic methods could be not enough effective and precise. The experimental data for $\omega_{dR/R} - \omega_B$ should be fitted by $\partial\varphi_\eta / \partial t$, which follows from Eqs. (11), (34) and (40), by using the fitting parameter $\varepsilon \mathrm{Re}$. When the initial pulse profile is well described theoretically while the effective viscosity b is known from the measurements of the linear sound absorption and velocity, the fits provide the value of $\varepsilon\upsilon_a$. Finally, to estimate the nonlinear parameter ε, the acoustic pulse amplitude υ_a should be measured independently or estimated theoretically with the knowledge of the linear physical properties of the materials.

3.6. Brillouin scattering by the bipolar coherent acoustic pulses

The solution presented in Eqs. (11), (34) and (40) is valid for the sequences of the rectangular acoustic pulses of arbitrary polarity. The particular solution in Eq. (41) describes the evolution of a single uni-polar acoustic pulse, which can be in practice emitted from a thin light absorbing film in the cases when the film is either perfectly matched in terms of acoustic impedance with the surroundings at its both faces, or when the film is perfectly matched with the substrate on one face while the other face of the film is loaded by a material with much higher (infinite) impedance. In the limiting case $\varepsilon \mathrm{Re} >> 1$ the evolution predicted by Eqs. (34), (41) and the Brillouin signal predicted by Eq. (11) are qualitatively similar to those predicted for the uni-polar acoustic pulses by the asymptotic methods of the analysis in Sections 3.1 -3.4.

Another common experimental situation is the case where one face of the film is in contact with the substrate while the other face is mechanically free, i.e., it is loaded by air with negligibly small acoustic impedance. In the limiting case of the perfectly matched film and the substrate, the coherent acoustic pulse launched in the substrate is bi-polar composed of two rectangular pulses of the opposite polarity. The analysis of the evolution of this pulse in the regime $\varepsilon \mathrm{Re} >> 1$ by the asymptotic methods described in Sections 3.1-3.4 provides insight on what additional phenomena could be expected, at least qualitatively, in the case of an arbitrary sequence of the rectangular pulses of varying polarity described in Section 3.5. We will not present here the complete approximate analysis which can be conducted along the lines presented in Sections 3.1 - 3.4, but we will just mention the most important difference between the uni-polar pulses (see Fig. 2) and the multi-polar acoustic pulses (see Fig. 4).

In the multi-polar pulses multiple shock fronts could be developed in the regime $\varepsilon \mathrm{Re} >> 1$ or just exist initially due to the specific opto-acoustic generation process. Then it could be expected that the time-resolved reflectivity measurements will be sensitive to all shock fronts and, generally, the time-resolved Brillouin oscillation will be more complicated due to the interference between the contributions to the total signal from all shock fronts. This is true except for perfectly symmetric bi-polar acoustic pulse, which presents opportunity for drastic simplification of the results due to the assumed symmetry. For example, at times scales, when for a uni-polar pulse in Sections 3.1-3.4 the Brillouin signal in Eq. (25) is due to probe scattering by a shock front with the amplitude $\varepsilon\upsilon_a(t)/2$ located in the sonic coordinate frame at $\xi = \xi_{sh}(t)$, while the light scattering from the trailing edge of the pulse is negligible, the signal from the bi-polar pulse will contain addition contribution accounting for the second shock front with the amplitude $-\varepsilon\upsilon_a(t)/2$ located at $\xi = -\xi_{sh}(t)$. The spectrum of the strain can be obtained using Eq. (26) with $\partial\upsilon/\partial\xi = -\upsilon_a\left[\delta(\xi+\xi_{sh}(t))+\delta(\xi+\xi_{sh}(t))\right]$

$$\tilde{\eta}_{zz}(t, q = 2k) = i\,\frac{\upsilon_a(t)}{kc_0}\cos\left[2k\xi_{sh}(t)\right]. \tag{42}$$

The solution in Eq. (42) reveals an important qualitative difference which could be expected in some cases of multi-polar pulses in comparison with the case of a uni-polar acoustic pulse. It can be seen that in the case of a perfectly symmetric bi-polar pulse the nonlinear processes and the shock front motion do not manifest themselves by the variations in frequency of the reflectivity oscillations because the unrapped phase of the signal (42) does not depend on time, $\varphi_\eta = const$, and, consequently, $\omega_{dR/R} = \omega_B$. The nonlinear processes manifest themselves as an additional modulation, proportional to $\left|\cos\left[2k\xi_{sh}(t)\right]\right|$, of the Brillouin amplitude, which is superimposed on the asymptotic dependence $A_\eta(t) \propto \upsilon_a(t)$. Thus the access to the nonlinear parameter in this case is through the measurements of the variations with time of the amplitude of the oscillation in transient reflectivity signal. It is worth mentioning that in the regime, currently under consideration, $2k\xi_{sh}(t)$ coincides with the parameter $\Lambda(t)$ introduced in Eqs. (27) and (28) in Section 3.2. In accordance with Eqs. (27) and (28) the additional modulations of the reflectivity signal due to the light scattering by the trailing front of the positive phase and the leading front of the negative phase of a bi-polar pulse can be important when $\Lambda(t) \le 1$. For $\Lambda(t) \ge 1$ the oscillatory character of the amplitude modulation in Eq. (42) could be important. So for the convenience it is worth to combine these predictions in a single formula. For the bipolar pulse described $\upsilon = \upsilon_a(t)\left[(\xi / \xi_{sh}(t)\right]H(\xi + \xi_{sh}(t))\left[1 - H(\xi - \xi_{sh}(t))\right]$ we derived from Eq. (11) that

$$\tilde{\eta}_{zz}(t, q = 2k) = i\frac{\upsilon_a(t)}{kc_0}\left\{\cos\left[2k\xi_{sh}(t)\right] - \frac{\sin\left[2k\xi_{sh}(t)\right]}{2k\xi_{sh}(t)}\right\}. \tag{43}$$

4. Comparison of the theoretical predictions with the experimental observations

In this Section we apply the developed theory to the interpretation of results obtained from conventional picosecond laser ultrasonics experiments. In these experiments the formation of weak shock fronts was expected during the propagation of the picosecond acoustic pulses.

4.1. Spatially resolved Brillouin scattering technique

The time-dependent amplitude oscillation of a time-resolved Brillouin scattering signal as predicted by Eq. (43) for bi-polar nonlinear acoustic pulses can be measured experimentally though observing the oscillation in space. This is possible because the modulation of the Brillouin scattering amplitude in time is equivalent to its modulation in space. Therefore, it is sufficient to substitute $t \Rightarrow z / c_0$ in the derived theoretical formulas. Recently, these spatial modulations have been experimentally observed in picosecond laser ultrasonics by detection of ordinary, i.e., stationary, Brillouin scattering of continuous light at multiple spatial positions along the propagation path of coherent picosecond acoustic pulses propagating in a sapphire sample.[24] In these experiments, a coherent strain pulses was generated in a 100 nm chromium film with one mechanically free surface. For such a 100 nm chromium film the characteristic initial duration of the acoustic pulse is $\tau_a \equiv H_f / c_f \approx 17$ ps. The nonlinearity of sapphire is characterized by the following nonlinearity constant[37]: $2\rho_0 c_0^2 \varepsilon = 18.3 \times 10^{11}$ N/m^2 ($\varepsilon \approx 1.82$); while the effective viscosity at room temperature is assumed to be[24] $b = 4.54 \times 10^4$ sN/m^2. For room temperature experiments[24] and using a strain amplitude of $M_a = \upsilon_a / c_0 \approx 10^{-3}$ we estimate $\varepsilon \,\mathrm{Re} \approx 68 >> 1$. From this estimate we conclude that the results of this experiment can be analyzed by the approximate methods described in Section 3. The characteristic nonlinear time is $t_{sh} = \tau_a /(\varepsilon M_a) \approx 9.3$ ns and the time it takes for the initially rectangular compression phase of the photo-generated pulse to transform into triangular form is $2t_{sh} =\approx 18.6\,\text{ns}$. It could be expected that the two shock fronts will be well defined at the times significantly shorter than $t_{sh}^{(2)} = 2(\varepsilon\,\text{Re}/4)^2 t_{sh} \approx 580 t_{sh} \approx 5.4\ \mu\text{s}$. Thus, we expect the amplitude modulation as described by Eq. (43) for the time window $20\,ns \le t \le 500\,ns$. Now, when we consider the sound velocity in sapphire as $c_0 = 11.23\times 10^3$ m/s, this time window will correspond to pulse propagation distances from approximately 0.2 mm to 5 mm, which exactly corresponds to the interval studied experimentally by Muskens and Dijkhuis[24]. For the used probe wavelength of 514 nm, the amplitude of the transient reflectivity signal starts to drop faster than predicted by Eq. (43) at the end of this observation interval because of the broadening of the shock fronts as described by Eq. (31). However, both, our analytical estimates and the numerical modeling of the solutions of the Burger's equation (considering the conditions from Ref. 24), confirm the existence of well-defined fronts for bipolar acoustic pulses up to a propagation distance of 5 mm. Thus, we attribute this experimentally observed oscillatory modulation of the scattered-light amplitude to the fact that under these conditions the light is predominantly scattered by two shock fronts moving in the sonic co-ordinate frame with equal, but oppositely directed velocities. The oscillatory modulation is a result of the continuous increase in the phase difference between these two signal contributions.

4.2. Time-resolved Brillouin scattering technique

More recently[25] , results from time-resolved Brillouin scattering of nonlinear picosecond acoustic pulses in liquid were reported. Note that this is the detection technique explicitly assumed in our preceding theoretical analysis in Sections 2 – 6.. In those measurements, the photoexcitation of a H=33 nm thick aluminum film deposited onto a sapphire substrate and loaded by a liquid, DC704,[25,38] launched a train of acoustic pulses of alternating polarity and progressively diminishing amplitude into the liquid. The structure of the pulse is illustrated in Fig. 4. The duration of each of the alternating phases is equal to twice the time of longitudinal acoustic wave propagation across Al film. Thus, the characteristic duration of the phases at half-width-half-maximum can be estimated as $\tau_a = H/c_{Al} \approx 5.2\,\text{ps}$, where $c_{Al} \approx 6.4\cdot 10^3\,\text{m/s}$ is the sound velocity in Al. The relative amplitudes of the consecutive parts of the emitted acoustic wave are controlled by the reflection coefficients of sound at the Al-sapphire and Al-liquid interfaces , $R_1 \equiv R_{Al/sapphire}$ and $R_2 \equiv R_{Al/DC704}$, respectively. Using $R_1 \cong 0.45$, $R_2 \cong -0.75$, we estimate the shape of the acoustic pulse shown in Fig. as $\upsilon_{a2}/\upsilon_{a1} = R_1 \cong 0.45$, $\upsilon_{a3}/\upsilon_{a1} = R_1 R_2 \cong -0.34$, $\upsilon_{a4}/\upsilon_{a1} = R_1^2 R_2 \cong -0.15$, $\upsilon_{a5}/\upsilon_{a1} = R_1^2 R_1^2 \cong 0.12$.

The characteristic time τ_D at which the thermal diffusion in Al is supersonic[2,28] can be estimated as $\tau_D = D_{Al}/C_{Al}^2 \approx 1.1$ps, where $D_{Al} \cong 4.5 \cdot 10^{-5}$ m^2/s is the thermal diffusivity of Al. At times $t \geq \tau_D$ the thermal diffusivity is subsonic and has weak influence on the profiles of thermo-elastically generated acoustic pulses.[1,2,28] Under the conditions of the experiment[25] τ_D is an order of magnitude shorter than the full duration, $2\tau_a = 2H/c_{Al} \approx 10.4$ ps, of each of the alternating acoustic phases. That is why it is reasonable in the first approximation to neglect the contribution to the leading compression phase of the emitted pulse train in Fig. 4 of the acoustic waves emitted in the process of the Al film cooling, as it had been *apriori* assumed when plotting Fig. 4. The signal profile in Fig. 4 includes only the acoustic waves generated due to laser heating of Al film.

In the experiments[25] the probe laser radiation had been incident on Al film from the liquid side and the detected oscillating in time contribution to probe reflectivity $dR(t)/R$ is mostly due to the interference between the probe radiation reflected by the Al film and reflected by the hypersound launched in liquid. The Brillouin frequency $f_B = \omega_B/(2\pi) \cong 40$ GHz had been measured at low pump laser fluence $F_L \leq 0.2$ mJ/cm^2, where it had been observed that the frequency $\omega_{dR/R}$ of the oscillating component of transient reflectivity does not depend on pump laser fluence. The major result of the experiment[25] is the reported dependence of the frequency $\omega_{dR/R}$ of the oscillating component of the transient reflectivity $dR(t)/R$ both on pump laser fluence and on time in the experimentally tested ranges 0.29 mJ/cm2$\leq F_L \leq 10.3$ mJ/cm^2, 100 ps $\leq t \leq 2000$ps, corresponding to more than 35 times increase in laser fluence and an order of magnitude wide window in the time domain.

In accordance with the theory developed above in Section 3 the analysis of the experimental data should be started by estimating the characteristic parameter $\varepsilon \mathrm{Re}$, the product of the nonlinear acoustic parameter and of the acoustic Reynolds number, which determines the regime of the emitted acoustic wave evolution in time and space. In the experiment the relative deviation $(\omega_{dR/R} - \omega_B)/\omega_B$ of the detected oscillation frequency from the linear Brillouin frequency in the beginning of the evaluated time interval, *i.e.*, at *t*=100 ps, is reported to be $0.002 \leq (\omega_{dR/R} - \omega_B)/\omega_B \leq 0.072$. These values can be used to estimate the product εM_a of the acoustic nonlinear parameter and of the acoustic Mach number, by assuming that the deviation of $\omega_{dR/R}$ from ω_B are caused by the supersonic propagation of the weak compression shock related to the leading compression phase of the acoustic signal presented in Fig. 4. In accordance with Eq. (25), we use for the estimates the relation $(\omega_{dR/R}-\omega_B)/\omega_B \approx \varepsilon M_a(t)/2$. Consequently, at t=100 ps we can estimate $0.004 \le \varepsilon M_a \le 0.144$. Using the definition of the acoustic Reynolds number,[23] $\mathrm{Re} \equiv 2\rho_0 c_0 \upsilon_a \tau_a / b$, and the knowledge of sound absorption coefficient $\alpha = \alpha(\omega)$ in DC704 at considered frequencies and temperatures[25] $\alpha(\omega) = b\omega^2/(2\rho_0 c_0^3) = \Gamma / c_0$, with $\Gamma \cong 2$ ns^{-1} at the experimental temperature of 200°K, we present $\varepsilon\,\mathrm{Re}$ in the form $\varepsilon\,\mathrm{Re} = \varepsilon M_a \omega_B^2 \tau_a / \Gamma$. Thus for 0.29 mJ/cm$^2 \le F_L \le$ 10.3 mJ/cm^2 at t=100 ps it can be estimated that $0.63 \le \varepsilon\,\mathrm{Re} \le 23$. It is important that these estimates demonstrate that for $F_L \ge 4.4$ mJ/cm^2 the non-dimensional parameter $\varepsilon\,\mathrm{Re} \ge 10 >> 1$ and, theoretically, the evolution of the leading compression phase of the acoustic signal in Eq. (4) can be described not by the Burgers equation, Eq. (10), but by the simple-wave equation, Eq. (14), which describes the dynamics of delta-localized shock fronts.

In accordance with the theory presented in Section 3 the largest in amplitude weak compression shock front is expected in the evolution of the leading compression phase, for which the above estimates have been conducted. The largest in amplitude dilatation shock front could be formed at the trailing edge of the second (dilatation) phase of the acoustic signal in Fig. 4. However, in accordance with our estimates the amplitude of the dilatation shock would be at least $\upsilon_{a1}/(\upsilon_{a5}-\upsilon_{a4}) \approx 4$ times smaller than of the compression shock, the condition $\varepsilon\,\mathrm{Re} >> 1$ does not hold even at the highest pump laser fluences, and, consequently, the dilatation shock will be importantly additionally suppressed relative to the compression one by the acoustic absorption.

The conducted estimates indicate that under the conditions of the considered experiment it is worth trying to model transient Brillouin reflectivity signal by assuming that it is due only to the first leading compression phase of the acoustic pulse train. Moreover, assuming that the compression pulse in the interval $\xi_3 \le \xi \le 0$ (see Fig. 4), which is composed of two rectangles, is transformed due to nonlinear acoustic process in a triangular shape pulse at time scales $\tau_{sh} \le 100$ ps, the experimental data can be fitted in the complete observation window 100 ps $\le t \le$ 2000ps by the formulas derived in Sections 3.1 - 3.4 for the triangular pulses. Neglecting in Eq. (28) the modulation of $(\omega_{dR/R}-\omega_B)/\omega_B$ due to the probe light reflection from the trailing edge of the triangular pulse, the fitting formula can be presented in the form

$$\frac{\omega_{dR/R}-\omega_B}{\omega_B} \cong \frac{\varepsilon M_a(t)}{2} \cong \frac{(\varepsilon M_a/2)}{\sqrt{1+(\varepsilon M_a/2)(t/\tau_a)}}\,. \qquad (44)$$

Here $M_a = \upsilon_a / c_0$ is the initial, *i.e.*, at *t*=0, Mach number of the equivalent triangular pulse. The initial amplitude υ_a of the triangular pulse is related to the initial amplitude υ_{a1} of the leading phase in the signal presented in Fig. 4 by the law of the pulse area conservation, i.e., $\upsilon_{a1}\tau_a + \upsilon_{a2}\tau_a = (1+R_1)\upsilon_{a1}\tau_a = \upsilon_a\tau_a$. Consequently, $\upsilon_a = (1+R_1)\upsilon_{a1}$ and $\varepsilon M_a = (1+R_1)\varepsilon M_{a1} \approx 1.45\varepsilon M_{a1}$. The fits with Eq. (44) were conducted [25], by adjusting the parameters εM_a and τ_a, all the experimental dependences measured for 0.29 mJ/cm^2$\leq F_L \leq 10.3$ mJ/cm^2. Even visually the quality of the fits continuously increases with the increasing pump laser fluence due to the increasing characteristic acoustic Reynolds number, as it could have been previewed from the theory and the estimates. At fluences $F_L \geq 4.4$ mJ/cm^2, where validity of Eq. (44) is expected, the dependence of the acoustic Mach number and the initial duration of the compression pulse can be well approximated by

$$\varepsilon M_a \cong 0.035(F_L /[mJ/cm^2]),\ \tau_a^{fit} \cong 5.5\ ps. \qquad (45)$$

The close proximity of the τ_a^{fit} to the theoretically expected value $\tau_a = H / c_{Al} \approx 5.2$ ps is a strong support for the validity of the theoretical model in Eq. (44). Moreover, using Eq. (45) it is straightforward to estimate that the characteristic time of the triangular pulse formation, $\tau_{Sh} \equiv (c_0\tau_a)/(\varepsilon\upsilon_{a1}) = (1+R_1)\tau_a /(\varepsilon M_a)$, is shorter than 100 ps for $F_L \geq 2.4$ mJ/cm^2. It is also possible to estimate, by using Eq. (30), that the finite width of the shock front, $\Delta\xi_{sh}(t)$, which is controlled by the competition of the nonlinearity and dissipation, is shorter than the initial duration τ_a of the acoustic pulse even at the end of the experimental time window, *i.e.*, at t=2000 ps, for $F_L \geq 4.3$ mJ/cm^2. Finally, it should not be forgotten, that in the model of Eq. (45), in comparison with more precise description in Eq. (28), the modulation provided by the function $\Xi(\Lambda(t))$ and presented in Fig. 3 (b) has been omitted. In accordance with the plot in Fig. 3. (b) the effect of this additional modulation is smaller than 10% for $\Lambda(t) \geq \pi$. This inequality is equivalent to $\tau_a(t) = \tau_a\sqrt{1+(\varepsilon M_a / 2)(t / \tau_a)} \geq \pi /(2\omega_B) \approx 6.2$ ps. Using Eq. (45) we estimated that the additional modulation provided by the probe light reflection from the trailing edge of the compression pulse is negligible at time scales $t \geq 100$ ps for pump fluences $F_L \geq 1.9$ mJ/cm^2.

On the basis of the above presented estimates and good quality of the fits it can be concluded that the deviation of the frequency $\omega_{dR/R}$ of the oscillating contribution to transient reflectivity from the linear Brillouin frequency ω_B for $F_L \geq 4.4$ mJ/cm^2 in the experiments [25] is due to the supersonic propagation of the weak compression shock front. Moreover the dynamics of the weak acoustic shock front evolution at picoseconds – nanosecond time scale can be described by the classical formulas of the nonlinear acoustics. The experimentally determined dependence in Eq. (45) of the product εM_a on the pump laser fluence can be used for the evaluation of the nonlinear acoustic parameter of liquids in GHz frequency range if the dependence of the acoustic Mach number on laser fluence is modeled theoretically from the thermo-elastic sound generation problem or measured experimentally (for example by monitoring optically the displacement of the Al/sapphire interface at picosecond time scales).

5. Conclusions

We presented an analytical theory describing how the nonlinear reshaping of a propagating, finite amplitude picosecond acoustic pulse results in the time-dependence of the observed Brillouin frequency and amplitude in a time-resolved Brillouin scattering experiment. In particular, the conditions, under which the detected frequency provides information on time-evolving speed of the weak-shock front or fronts that can be formed through the nonlinear acoustic transformation of the strain pulse, are established. Depending on the parameters of the initial strain pulse and the monitored time interval of its nonlinear transformation, our theory predicts the detected frequency to either be monotonically decreasing or oscillating in time. We also predicted the influence on the Brillouin scattering signal of the linear acoustic absorption which could broaden with time/distance the widths of the propagating shock fronts. We highlighted different behaviours of the Brillouin signals in case of uni-polar and bi-polar nonlinear acoustic strain pulses. We presented examples how the developed theory can be successfully applied for interpretation of available experimental data, providing access to the evaluation of the nonlinear acoustic properties of the media in the GHz frequency range.

Acknowledgements

The author is grateful to Christophe Klieber for the help in preparation of the figures and fruitful discussions and to keith Nelson and Thomas Pezeril for fritful discussions. The author acknowledge the support in the frame of the project ANR BLANC 2012 “PLUSDIL”.

References

[1] C. Thomsen, H. T. Grahn, H. J. Maris, and J. Tauc, Phys. Rev. B **34**, 4129 (1986).

[2] S. A. Akhmanov and V. E. Gusev, Sov. Phys. Uspekhy, 35, 153-191 (1992)

[3] H. T. Grahn, H. J. Maris, and J. Tauc, IEEE QE **25**, 2562 (1989).

[4] H. –N. Lin, R. J. Stoner, H. J. Maris, and J. Tauc, J. Appl. Phys. **69**, 3816 (1991).

[5] V. Gusev, Acustica Acta Acustica **82**, S37 (1996).

[6] J. W. Tucker and V. W. Rampton, *Microwave Ultrasonics in Solid State Physics* (North-Holland Publ. Co., Amsterdam, 1972).

[7] C. Mechri, P. Ruello, J. M. Breteau, M. R. Baklanov, P. Verdonck, V. Gusev, Appl. Phys. Lett. **95**, 091907 (2009).

[8] O. B. Wright and T. Hyoguchi, Opt. Lett. **16**, 1529 (1991).

[9] O. B. Wright, J. Appl. Phys. **71**, 1617 (1992).

[10] P. Babilotte, P. Ruello, D. Mounier, T. Pézeril, G. Vaudel, M. Edely, J.-M. Breteau, V.Gusev, K. Blary, Phys. Rev. B **81**, 245207 (2010).

[11] C. Mechri, P ; Ruello, V. Gusev, New J. Phys. 14, 023048 (2012).

[12] O. Matsuda, O. Wright, D. Hurley, V. Gusev, K. Shimizu, Phys. Rev. Lett. **93**, 095501 (2004).

[13] R. Cote, A. Devos, Rev. Sci. Instrum. **76**, 053906 (2005).

[14] C. Mechri, P. Ruello, V. Gusev, J.-M. Breteau, D. Mounier, M. Henderson, A. Gibaud, S. Dourdain, Eur. Phys. J. Special Topics **153**, 211 (2008).

[15] A. M. Lomonosov, A. Ayouch, P. Ruello, G. Vaudel, M. R. Baklanov, P. Verdonck, L; Zhao, V. E. Gusev, ACSNano **6**, 1410 (2012).

[16] V. Gusev, A. M. Lomonosov, P. Ruello, A. Ayouch, G. Vaudel, J. Appl. Phys. **110**, 124908 (2011).

[17] B. Perrin, B. Bonello, J. C. Jeannet, E. Romatet, Prog. Nat. Sci. **S6**, 444 (1996).

[18] D. H. Hurley, O. B. Wright, Opt. Lett. **24**, 1305 (1999).

[19] O. Matsuda, O. B. Wright, D. H. Hurley, V. Gusev, K. Shimizu, Phys. Rev. B **77**, 224110 (2008).

[20] D. Mounier, E. Morozov, P. Ruello, M. Edely, P. Babilotte, C. Mechri, J.-M. Breteau, V.

Gusev, J. Phys.: Conf. Ser. 92, 012179 (2007).

[21] D. Mounier, E. Morozov, P. Ruello, J.-M. Breteau, P. Picart, V. Gusev, Eur. Phys. J. Special Topics **153**, 243 (2008).

[22] D. Mounier, P. Picart, P. Babilotte, P. Ruello, J.-M. Breteau, T. Pézeril, G. Vaudel, M. Kouyaté, V. Gusev, Optics Express **18**, 6767 (2010).

[23] O. V. Rudenko and S. I. Soluyan, *Theoretical Foundations of Nonlinear Acoustics* (Consultant Bureau, New York, 1977).

[24] O. L. Muskens, J. I. Dijkhuis, Phys. Rev. Lett. **89**, 285504 (2002).

[25] C. Klieber, Ph.D. Thesis, http://hdl.handle.net/1721.1/57801, MIT (2010) ; V. Gusev, C. Klieber, T. Pezeril, K. Nelson, 2013 International Congress on Ultrasonics, Singapore, Program and Abstracts (page 21).

[26] J. F. Nye, *Physical Properties of Crystals* (Oxford Univeristy press, Oxford, 1957).

[27] P. M. Morse, *Theoretical Acoustics* (Princeton University Press, Princeton, 1968).

[28] V. E. Gusev and A. A. Karabutov, *Laser Optoacoustics,* Chapter 6 (AIP, New York, 1993).

[29] V. Gusev, J. Acoust. Soc. Am, **107**, 3047 (2000).

[30] V. Gusev, B. Wu, G. J. Diebold, J. Appl. Phys. **110**, 044908 (2011).

[31] G. W. Collins et al., Science **281**, 1178 (1998).

[32] P. M. Celliers, G. W. Collins, L. B. Da Silva, D. M. Gold, R. Cauble, Appl. Phys. Lett. **73**, 1320 (1998).

[33] D. K. Bradley et al., Phys. Rev. Lett. **93**, 195506 (2004).

[34] A. Ravasio et al., Phys. Rev. Lett. **99**, 135006 (2007).

[35] S. Root et al., Phys. Rev. Lett. **105**, 085501 (2010).

[36] S. D McGrane, D. S. Moore, D. J. Funk, J. Appl. Phys. **93**, 5063 (2003).

[37] H.-Y. Hao, H. J. Maris, Phys. Rev. B **64**, 064302 (2001).

[38] C. Klieber, T. Pezeril, S. Andrieu, K. A. Nelson, J. Appl. Phys. 112, 013502 (2012)

Figures and captions

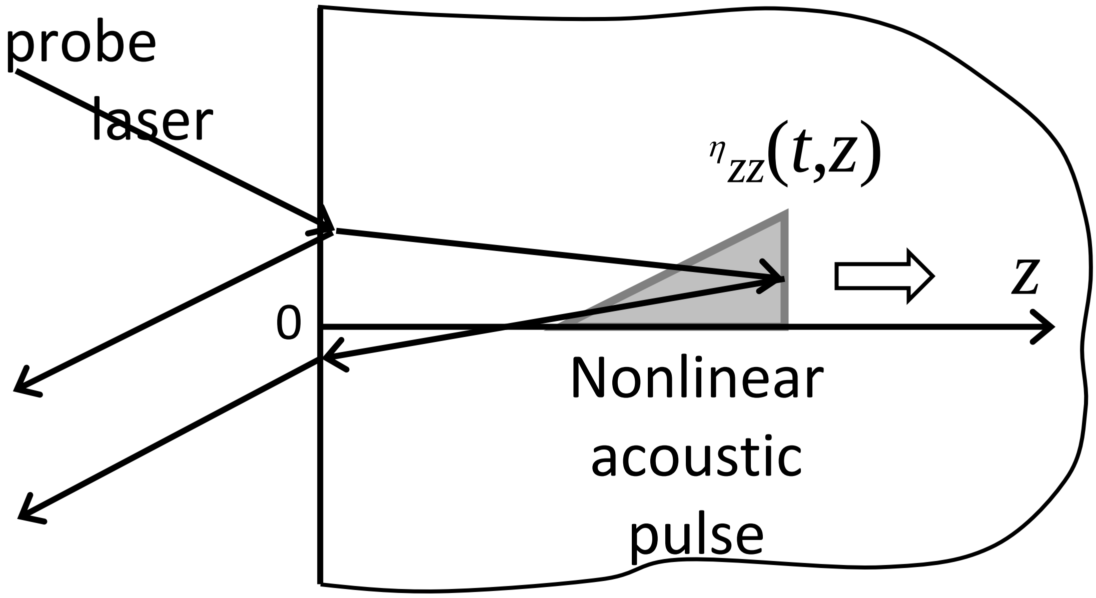

Figure 1

Physical principle of the picosecond acoustic interfermetry. Weak optical field reflected by the plane acoustic strain pulse propagating normally to the sample surface is heterodyned against stronger field reflected from the sample surface. When the acoustic pulse propagates at constant velocity, linearly changing in time phase shift between the two interfering reflected optical fields leads to sinusoidal variation with time of transient reflectivity changes.

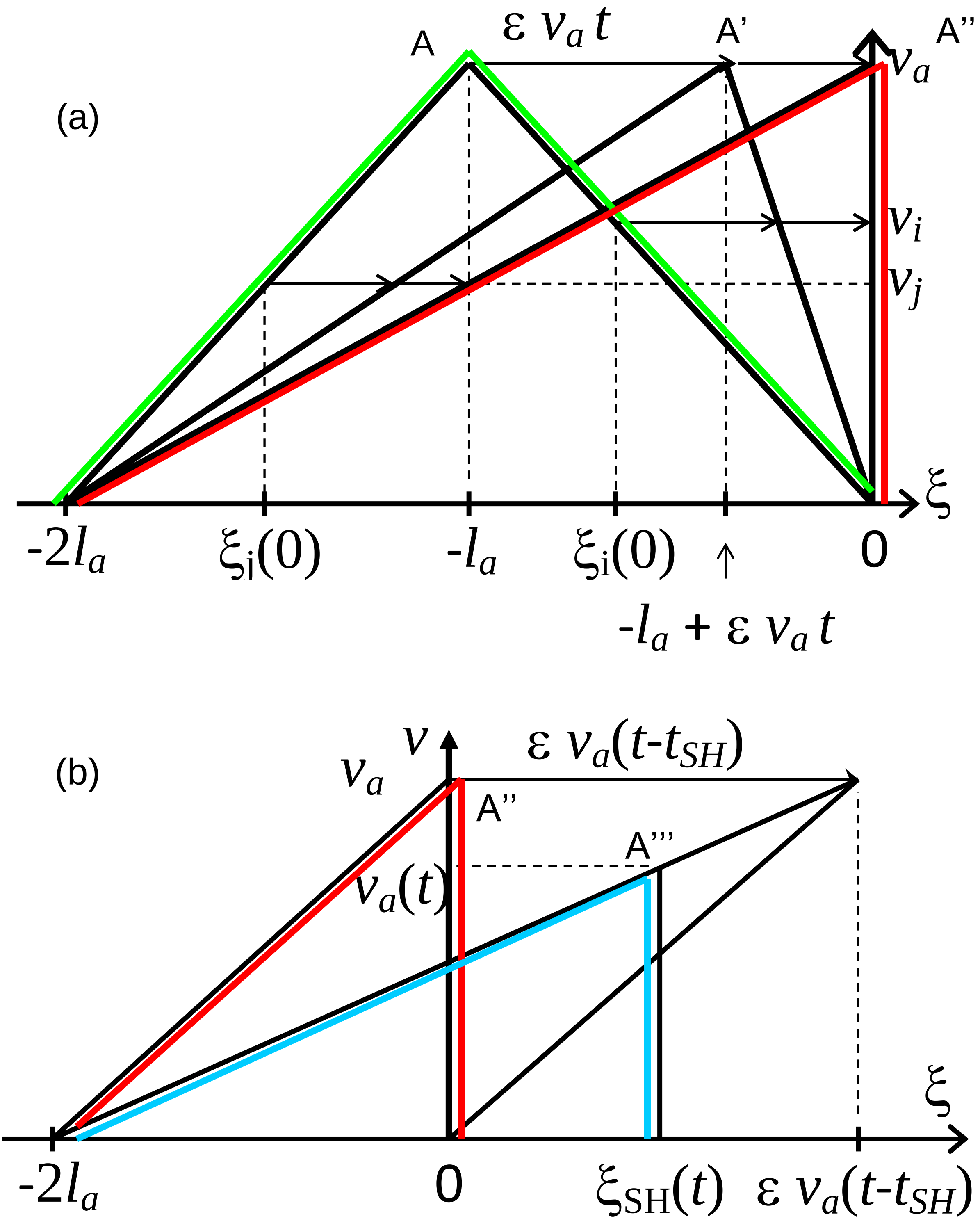

Figure 2. Transformation of the particle velocity profile of the triangular acoustic pulse of the finite amplitude in the frame of the quadratic approximation of the nonlinear acoustics. (a) All the points of the initial profile with the peak located in point *A* are displaced with increasing propagation time horizontally. These displacements are illustrated for some particular points by the

arrows. This leads first to the shortening of the leading front of the acoustic pulse (profile with the peak in point A') and later to formation of the shock front (profile with the peak in point A''). (b) After the formation of the shock front (profile with the peak in point A'') the amplitude of the acoustic pulse amplitude starts to diminish with increasing time (profile with the peak in point A''').

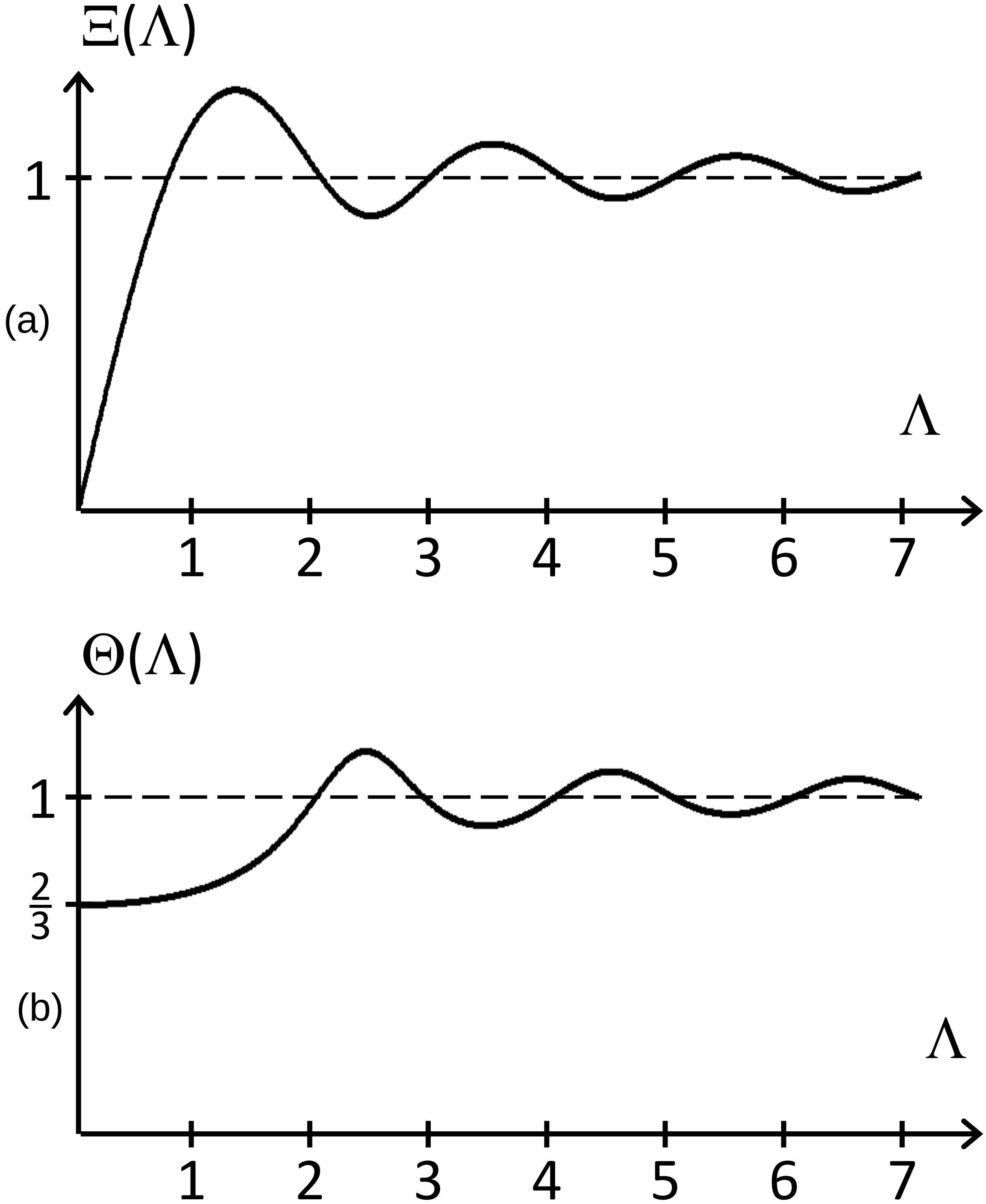

Figure 3

(a) The presentation of the function $\Xi(t) \equiv \sqrt{1-2\sin c(\Lambda)+\sin c^2(\Lambda/2)}$, describing transitional modulation of the Brillouin signal amplitude, which is superimposed on its asymptotic proportionality to the velocity of the shock front.

(b) The presentation of the function $\Theta(\Lambda) \equiv \frac{1 - \sin c(\Lambda)}{1 - 2\sin c(\Lambda) + \sin c^2(\Lambda/2)}$, describing transitional modulation of the frequency $\omega_{dR/R}$ of the transient reflectivity oscillation, which is superimposed on its asymptotic variation proportionally to the velocity of the shock front.

Here $\Lambda(t) \equiv 4kl_a(t)$ is the normalized length of the acoustic pulse, which starts to increase after the shock front formation. The modulations are due to the contribution of probe light scattered by the trailing long front of the acoustic pulse.

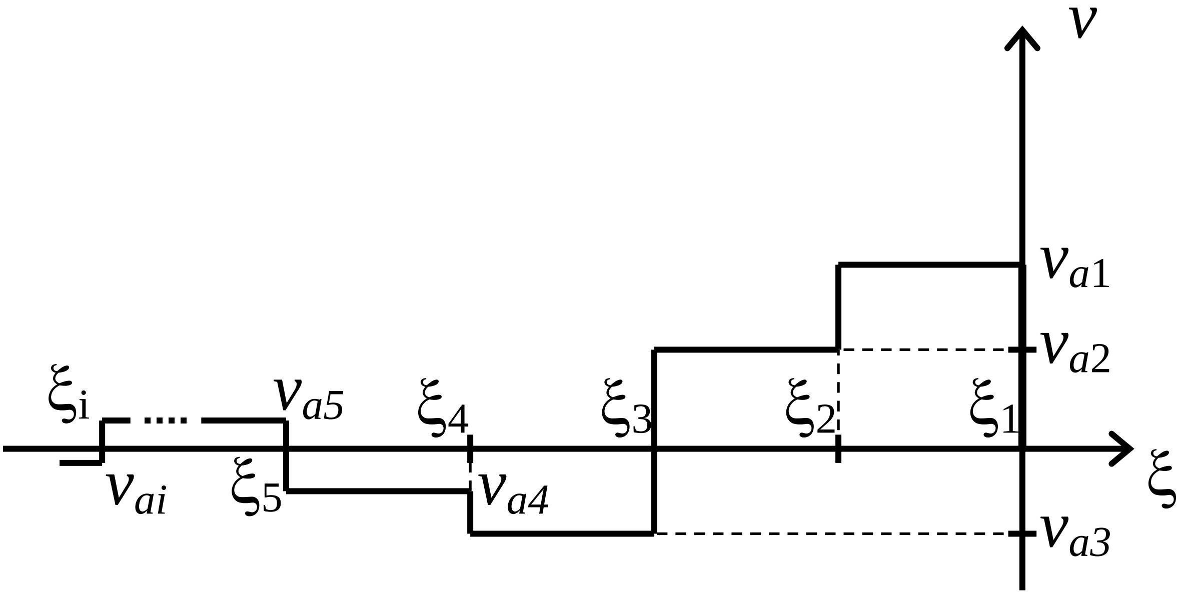

Figure 4

Presentation of the typical train of rectangular acoustic pulses emitted into the sample from thin metallic film sandwiched between the substrate and transparent loading material and heated by ultrasort laser pulse. It is assumed, for definiteness, that the acoustic impedance of the material is lower than that of the film, while the impedance of the film is lower than that of the loading.